Preliminary Modelling for the Stock Assessment of Shortfin Mako Shark, *Isurus oxyrinchus* using CMSY and JABBA

S. Bonhommeau[1], E. Chassot[2], J. Barde[3], P. de Bruyn[2], F. Fiorellato[2], L. Nelson[2], D. Fu[2], A.E. Nieblas[4]

[1] IFREMER, DOI, La Reunion, France

[2] IOTC, Seychelles

[3] IRD, France

[4] Company for Open Oceans Observations and Logging, La Reunion, France

Abstract

The shortfin mako shark, Isurus oxyrinchus (SMA), is a highly migratory pelagic species found globally. It is particularly vulnerable as bycatch in longline fisheries, and has a vulnerable status according to the IUCN. SMA is considered a data-limited stock as there is incomplete catch information, limited information on the catch composition (size frequencies), and few abundance indices (e.g., standardised CPUE series). A preliminary stock assessment was performed by Brunel et al. in 2018 for the IOTC convention area using CMSY, a catch-only method, and a built-in Bayesian surplus production model (BSM), based on reconstructed catch data and standardised CPUEs from the EU longline fleet of Spain (2006-2016), and Portugal (2000-2016). This preliminary assessment found that SMA had been experiencing overfishing from the 1990s (F/Fmsy =2.57), but that the biomass of the stock was decreasing but not overfished (B2015/Bsmy close to 1). Here, we perform preliminary assessments using updated catch and CPUE indices for SMA. Contrary to Brunel et al, we use nominal catch of SMA (1964-2018) and scaled CPUEs from Japan (1993-2018), Spain (2001-2018), Taiwan (2005-2018), and Portugal (2000-2018). Catch ratio between SMA catch and target species catch as used in Brunel et al. were not available at the time of the stock assessment. We develop a demographic analysis based on Leslie Matrices to determine a prior for r (resilience, or intrinsic growth rate). We run JABBA (Winker et al. 2018) and CMSY, two surplus production models and compare these results to those of Brunel et al. 2018. We compare the outputs of CMSY to those of JABBA, providing background and advice in parameterising the model. We find that JABBA and CMSY give consistent results in terms of reference points, which indicate that SMA is experiencing overfishing (F/Fmsy well above 1) but is not overfished (most results indicate B/Bmsy > 1). As JABBA can take into account all CPUEs to inform the stock assessment, we define these model outputs as our best case scenario. The projections are run and provided for this model.

Introduction

The shortfin mako shark (SMA), Isurus oxyrinchus, is a highly-migratory pelagic species found in the global ocean. It inhabits the epi-pelagic to meso-pelagic zone (Caillet 2009) and is particularly vulnerable as bycatch in longline fisheries targeting swordfish and tuna (Caillet 2009), and a less frequent bycatch in purse seine fisheries. They are targeted in several areas of the Indian Ocean using hook and line, and gillnets. Its distribution overlaps intensive pelagic fisheries, and worldwide, it is the second most abundant bycatch shark species after blue shark, Prionace glauca, (IUCN 2007). It is listed as having a "vulnerable" status by the IUCN due to the high incidence of catch and its slow reproduction time (18-21 years for females to reach maturity) (Mollet et al. 2000, Cailliet 2009).

A preliminary stock assessment was performed by Brunel et al. 2018 in preparation for the full stock assessment of SMA planned for the 2020 WPEB. This preliminary assessment used the Catch at Maximum Sustainable Yield (CMSY) algorithm (version 2015, https://github.com/SISTA16/cmsy/tree/master/Legacy; Froese et al. 2016). To inform their models, they reconstructed catch of the SMA using a ratio factor of the catch data from the IOTC longline fisheries targeting both swordfish and tuna. They standardised CPUE indices provided by Spain and Portugal updated until 2016. They developed a demographic analysis based on Leslie matrices to derive an appropriate, r, (resilience or intrinsic growth rate). They explored a range of priors, and tested these using both the CMSY (catch-only) and the Bayesian state-space surplus production model (BSM) that is applied in the CMSY algorithm when abundance indices are available. Their outputs indicate that the SMA is experiencing overfishing, but that it is not overfished, with B/BMSY close to 1. They also note that the trend in biomass is decreasing.

Here, we conduct an updated stock assessment of the shortfin mako. Contrary to Brunel et al, we use nominal catch of SMA (1964-2018) and scaled CPUEs from Japan (1993-2018), Spain (2001-2018), Taiwan (2005-2018), and Portugal (2000-2018). Catch ratios between SMA catch and target species catch as used in Brunel et al. were not available at the time of the stock assessment. We develop a demographic analysis based on Leslie Matrices to determine a prior for r (resilience, or intrinsic growth rate). We use JABBA (Winker et al. 2018), a widely-used surplus production model, as well as CMSY to directly compare with the results of Brunel et al. 2018.

Both JABBA and CMSY are written in the R programming language and made available via Github (JABBA: github.com/jabbamodel/JABBA; CMSY: https://github.com/SISTA16/cmsy).

1. Stock assessment methods

1.1 CMSY

CMSY is a data-limited Monte-Carlo method of assessing fisheries reference points and relative stock size using catch data. It is parameterised based on species' life history characteristics (Froese et al. 2017). The

Schaefer production model parameters are r (resilience or intrinsic growth rate) and K (maximum stock size or carrying capacity), whose different combinations will produce different time series of biomass. In CMSY, the Schaefer model is run many times to calculate annual biomasses for r-K pairs randomly drawn from the prior distributions. The model determines which r-K pairs are valid: e.g., those pairs that result in a biomass time series that do not (1) result in a stock collapse or (2) allow the stock to exceed carrying capacity. Also, those r-K pairs that result in a final relative biomass estimate between the values specified in the inputs (the final depletion range), are accepted and used to calculate MSY (rK/4) and biomass over time. The geometric means of the resulting density distributions of r, K and MSY are taken as the most probable values. These values are then used to determine reference points for management.

When abundance indices are available, the CMSY algorithm runs an advanced Bayesian state-space implementation of the Schaefer surplus production model (BSM). The advantage of the BSM is that it is focused on informative priors and that it accepts short (minimum 3 years) and fragmented abundance data (Froese et al. 2015).

We use the 2015 version of the CMSY, though a new version was released in December 2019. Both versions can be downloaded from github (https://github.com/SISTA16/cmsy). A detailed user guide is available (Froese et al. 2015), which we follow throughout.

1.2 JABBA

The Bayesian state-space surplus production model framework JABBA (Winker et al., 2018, github.com/jabbamodel/JABBA), is used for this stock assessment as it provides a user-friendly R to JAGS interface for fitting generalized Bayesian State-Space SPMs with the aim to generate reproducible stock status estimates and diagnostics. JABBA's inbuilt options include:
- Automatic fitting of multiple CPUE time series and associated standard errors;
- Fox, Schaefer or Pella Tomlinson production function (optional as input Bmsy/K);
- Kobe-type biplot plotting functions;
- Forecasting for alternative TACs;
- Residual and MCMC diagnostics;
- Estimation or fixing of the process variance;
- Optional estimation of additional observation variance for individual or grouped CPUE time series.

In addition, JABBA provides extensive diagnostic procedures and associated plots (e.g. residual run tests) and a routine to conduct retrospective analysis. A full description of JABBA and codes are available on JABBA website.

2. Data requirements by method

2.1 CMSY

CMSY requires catch data and at least some biological information. `

The mandatory input fields for CMSY are
- Stock - fish stock name;
- yr - year of the catch
- ct - catch in tonnes
- bt - biomass estimates if available, e.g. CPUE, otherwise input "NA";

Other columns are identifiers that may be included, but are not necessary to run the model. CMSY requires that the catch time-series are at least 15 years from the start year to end year.

CMSY only allows for one abundance index to be included in each run of the analysis. Therefore, if several abundance indices are available, they must all be input in the 'bt' column, reproducing the same 'yr' and 'ct' information for each abundance index, but changing the 'Stock' name. Years with missing data should be filled with an 'NA' value.

2.2 JABBA model specifications

Data inputs required for JABBA are catch and abundance (e.g. CPUE time series) in .csv format. Standard errors (SE) for the time series can optionally be provided. These data are described in the data section below. Some biological information are required to define prior information on the intrinsic growth rate of the population r and the unfished equilibrium biomass K (see Setting priors by method).

The catch file contains time series of year and catch by weight aggregated across fleets for the entire fishery. Missing values are not allowed.

Multiple abundance indices from different sources can be included in a single file. This file must contain time series of year, which must match the years in the catch file. Missing or fragmented data are allowed.

The optional SE file must contain time series of year as in the catch and abundance files, and the standard error estimates of the abundance indices on a log scale. This option allows the user to apply weighting to individual abundance indices by assigning different coefficients of variation (CV) to each time series. The CV for each year should approximate the standard error on the log scale so that data weights match expectations of how well the models fit the data.

The csv input files should be named by joining the file type (i.e. 'catch', 'cpue', 'se') with the assessment name (e.g. SMA_SA) : catchSMA_SA, cpueSMA_SA, seSMA_SA. These files must be saved in a folder of the same name as the assessment name, e.g. /SMA_SA.

See the JABBA website for a full tutorial.

3. SMA stock assessment data

3.1 Biological information

Biological information is vital for properly informing the priors of both CMSY and JABBA, and can be found from a review of the literature, including past stock assessments.

SMA is a highly-migratory predator that preferentially inhabits open ocean areas globally, but is also present in coastal regions. Most biological information on the SMA comes from studies based in the western North Atlantic (Pratt and Casey 1983, Casey and Kohler 1992, Rosa et al. 2017), western and central Atlantic (Barreto et al. 2016), and the eastern (e.g. Klimley et al. 2002, Holts and Kohin 2003, and Sepulveda et al. 2004) and western Pacific (Bishop et al. 2006). Few biological data available from the Indian Ocean (e.g. south-western Indian Ocean Groeneveld et al. 2014) and no information is available about stock structure in the Indian Ocean, though it is noted that the SMA are distributed widely about the IOTC convention area (IOTC 2016).

In these other sites, SMA have an age-at-maturity of 18 to 21 years for females (Bishop et al. 2006, Natanson et al. 2006) and 7-9 years for males (Bishop et al. 2006). Their longevity is estimated to be between 29-31 years (Bishop et al. 2006, Natanson et al. 2006).

There is a large difference in size-at-maturity between the sexes. Over the different study sites, males have been found to mature between 195-215 cm (Pratt and Casey 1983, Stevens 1983, Cliff et al. 1990, Francis and Duffy 2005, Compagno 2001), and reach a maximum size of about 265 cm (Compagno 2001). Females, on the other hand, mature between 265-307 cm, with a maximum size of up to 400 cm and 570 kg. In the south-western Indian Ocean, females were estimated to mature at about 250 cm FL or at 15 years and 190 cm FL or 7 years for males (Groeneveld et al. 2014), and maximum sizes observed were 311.3 cm FL (not aged) for females and 299 cm (17 years) for males.

SMA are aplacental viviparous species whose developing embryos feed on the unfertilised eggs during gestation. Little is known about the reproductive pattern of this species, but it is believed that they gestate between 15-18 months, with a 3-year reproductive cycle (Mollet et al. 2000). Pupping and nursery grounds may be over shelf regions in the southwest Indian Ocean (Groeneveld et al. 2014). They produce between 4-25 pups, with 10-18 pups on average (Compagno 2001) with larger individuals producing more pups. They have a size-at-birth of between 60-70 cm.

3.2 Catch data

Catch data are required by both CMSY and JABBA.

Though SMA is a valuable target and bycatch species, catches are thought to be inadequately reported, and underestimated as landings are not thought to reflect the number of individuals finned and discarded at sea (IUCN 2007). Primary concern is that SMA are not sufficiently specified in the catch data (i.e. they are aggregated with other species). SMA is a mackerel shark, which may be listed in IOTC catch data as "Shortfin mako", "Mackerel sharks", "Mako sharks", "Sharks mackerel and porbeagles nei", "Sharks nei other than oceanic whitetip shark and blue shark", and "Sharks various nei". Mejuto et al. (2006) indicates that for the Spanish longline fleet, the label "Sharks various nei" (SKH) is primarily made up of blue shark and SMA.

Some concern has been expressed that the SMA can be misidentified as a longfin mako shark (LMA, Isurus paucus), though Mejuto et al. (2006) notes that identification as SMA is normally reliable as these fish are easily identified and often reported by the fleet themselves in their voluntary reports to categorise their catch for the market.

There is concern that the weight recorded for individuals refer to specimens that have already been processed, and do not reflect live weights (IOTC 2016). Mejuto et al. (2006) note that finning in the Spanish fleet, at least, declined rapidly in the mid-1980s, and thus the reporting of shark may be more representative of the actual catch after this period.

Considering the caveats listed above, the previous preliminary stock assessment performed by Brunel et al. (2018) reconstructed the catch based on the idea that SMA are caught in the swordfish and tuna fisheries at a fixed ratio. They thus reconstructed the SMA catch as the sum of the ratio of the 1) SWO longline fishery and 2) tuna longline fisheries. This method was originally described by Murua et al. 2013, having been developed via the European project EUPOA-Sharks. The method used in Brunel et al. (2018) corresponds to that described in Coehlo and Rosa (2017), who also based their method on that of Murua et al. (2013), but added a year stratification.

Here, we attempted to reconstruct the catch of SMA following the methods described in Coehlo and Rosa (2017). From the IOTC nominal catch, we extract SWO caught in the longline fishery targeting SWO (IOTC fishery code: ELL), which is used here as the SWO longline fishery. We then select the tuna species (BET, YFT, ALB) caught in the fresh (IOTC fishery code: FLL) and deep-freezing longline fisheries (IOTC fishery code: LL).
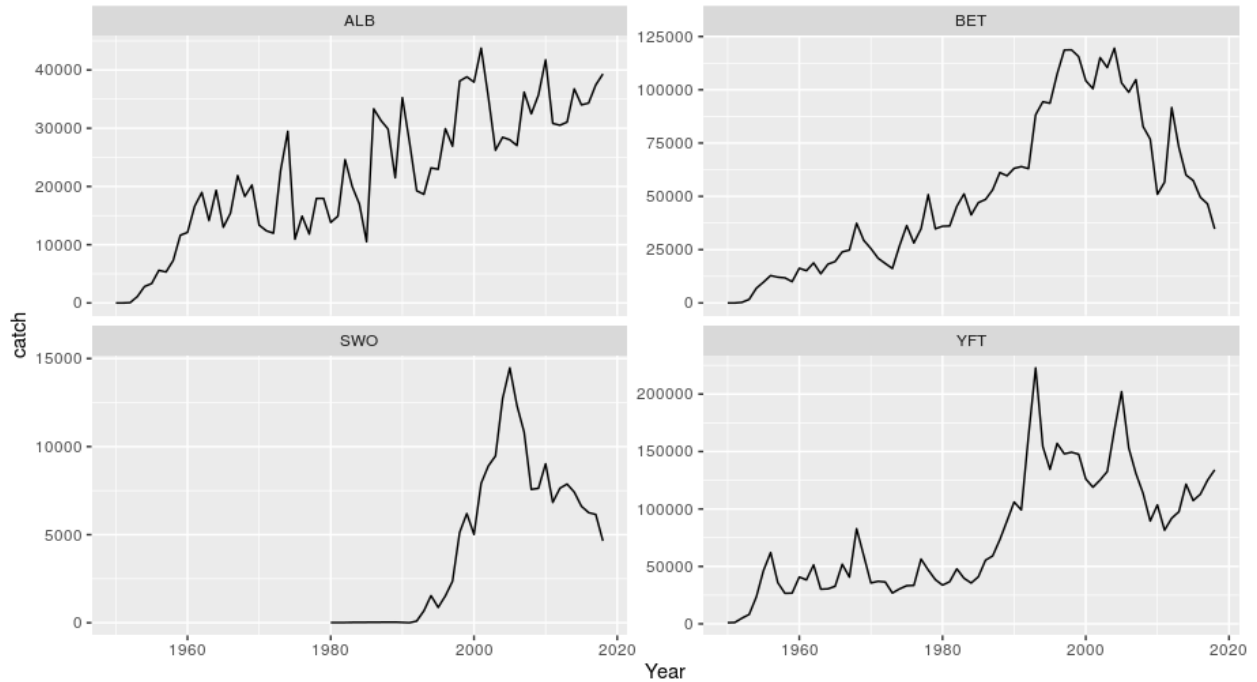
Figure 2. Original time series of the tuna species (*Thunnus alalunga*, albacore, ALB; *Thunnus obesus*, bigeye, BET; *Thunnus albacares*, yellowfin, YFT) targeted in the IOTC LL and FLL fisheries and swordfish (*Xiphias gladius*, SWO) from the IOTC ELL fishery, and from which the SMA catch was attempted to be reconstructed. Note that y-axes vary between plots.

Our catch reconstruction examined the ratios as defined in the IOTC supporting information (IOTC 2016), looking at a minimum, maximum, and mean of the ratios defined in Table 1. We were not able to reproduce nor approximate previous reconstructed time series (i.e. Figure 3).

Table 1. Estimated frequency of occurrence and bycatch mortality in the Indian Ocean pelagic fisheries (adapted from IOTC 2016 supporting info).

Gears	PS	LL		BB/TROL/HAND	GILL	UNCL
		SWO	Tuna			
Frequency	rare	common		rare–common	unknown	unknown
At-vessel mortality	unknown	13 - 56%	0 - 31%	unknown	unknown	unknown
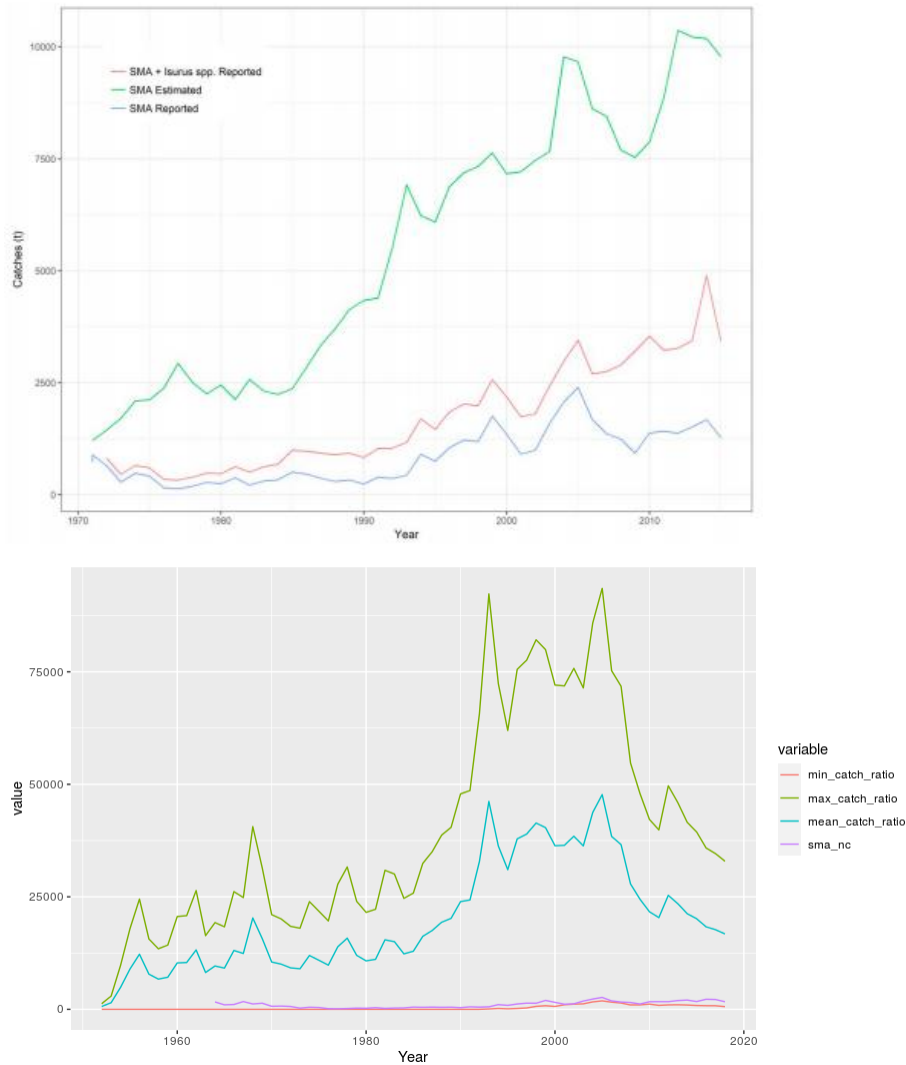
Figure 3. The catch reconstruction as found by Brunel et al. 2018 (top panel, green line), and the catch reconstruction found in this study based on the same methods (bottom panel, red, green, and blue lines).

Thus, though we note the caveats mentioned above in terms of SMA catch reporting, misidentification and multiple species aggregation, we decided to use the nominal catch data of SMA reported by CPCs to the IOTC (note that raised catches are not available for SMA; Figure 4). These catch data were downloaded from the IOTC WPEB16 website (https://iotc.org/meetings/16th-working-party-ecosystems-and-bycatch-wpeb16).
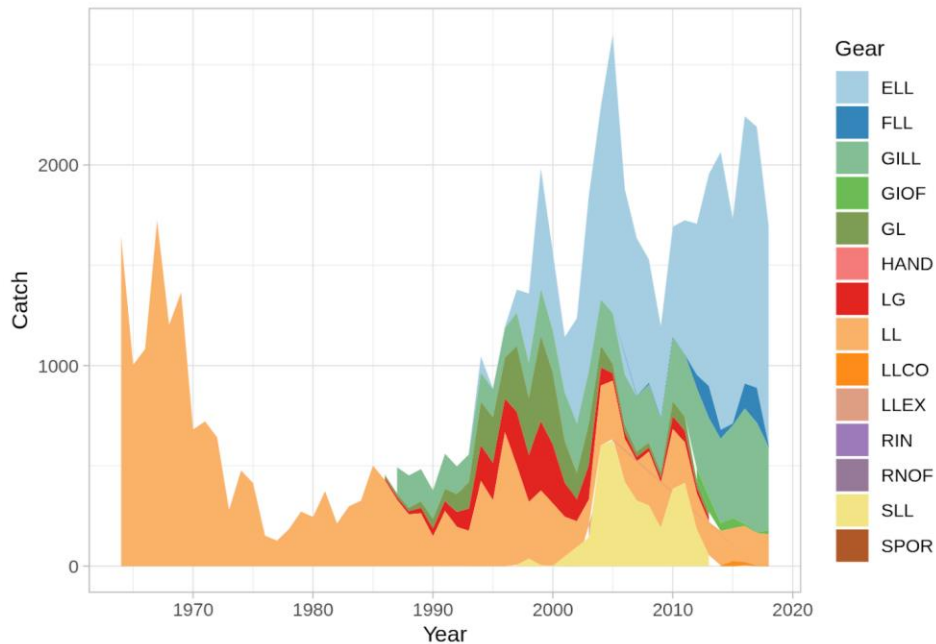
Figure 4. The catch in tonnes of SMA as reported by the CPCs to the IOTC (black line) and as reported via the IOTC Regional Observer Scheme (blue line). Both datasets are publicly-available for download on the IOTC website.

3.3 Abundance data

Abundance indices, e.g., CPUE, are an optional data input of CMSY and a required input of JABBA. The CMSY is a 'catch-only' model, but the CMSY algorithm should additionally apply a Schaefer Bayesian surplus production model (BSM) when abundance indices are available.

Four CPCs provided standardised CPUE indices, including Japan (Kai and Semba 2019), Taiwan,China (Tsai et al. 2019), EU,Spain (Ramos-Cartelle et al. 2020) and EU,Portugal (Coelho et al. 2020) with data updated to 2018. Both Spain and Portugal use a ratio factor in estimating their catch and calculating their CPUE as described above. Their standardised CPUEs have significantly higher absolute values than Japan and Taiwan (Figure 5). Thus, we have scaled all standardised CPUE indices to compare between the four different indices (Figure 6). No negative values are allowed for the CPUE indices in our methods, thus scaling was performed by dividing by the mean of each CPUE index (Figure 6; Table 2). The original CPUE indices and their confidence intervals as provided in the text of each of the CPC's working party documents can be found in Appendix 1.

CPUEs from EU,Spain, Taiwan,China and EU,Portugal show similar trends with increasing CPUE towards the end of the time series. Japan's index shows an opposing trend with high CPUE at the beginning of the time series, which then declines (Figure 5, Figure 6).

Here, we used the scaled CPUE indices as abundance indices for the models to facilitate comparison of model results.
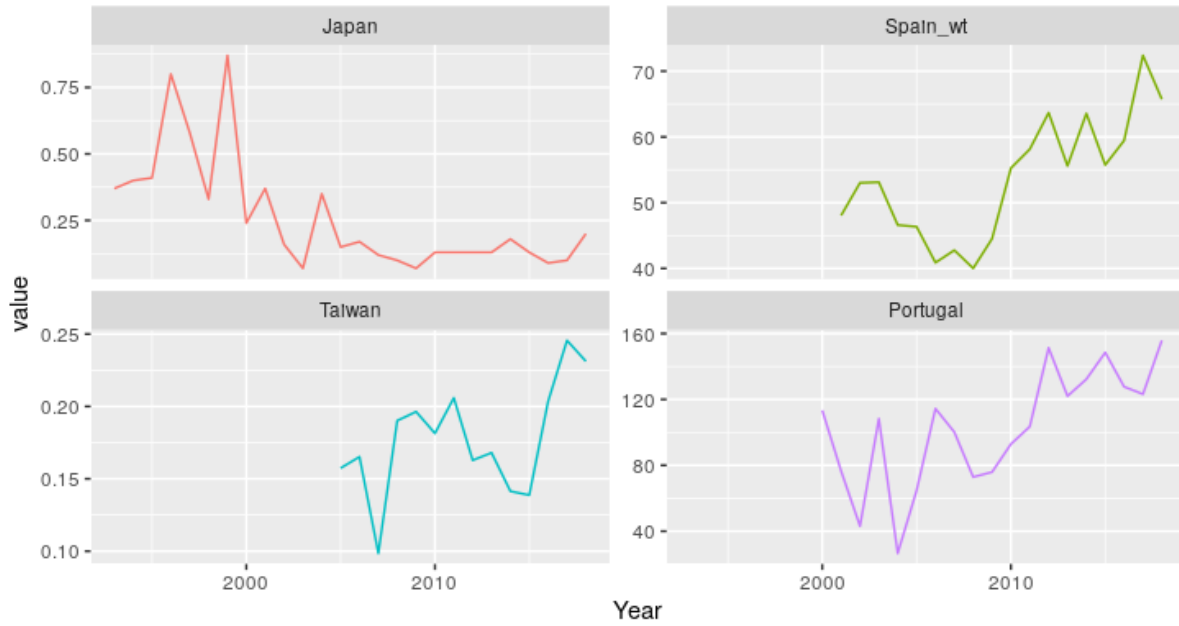
Figure 5. The standardised CPUE as reported to the IOTC by Japan, EU,Spain, Taiwan,China, and EU,Portugal.
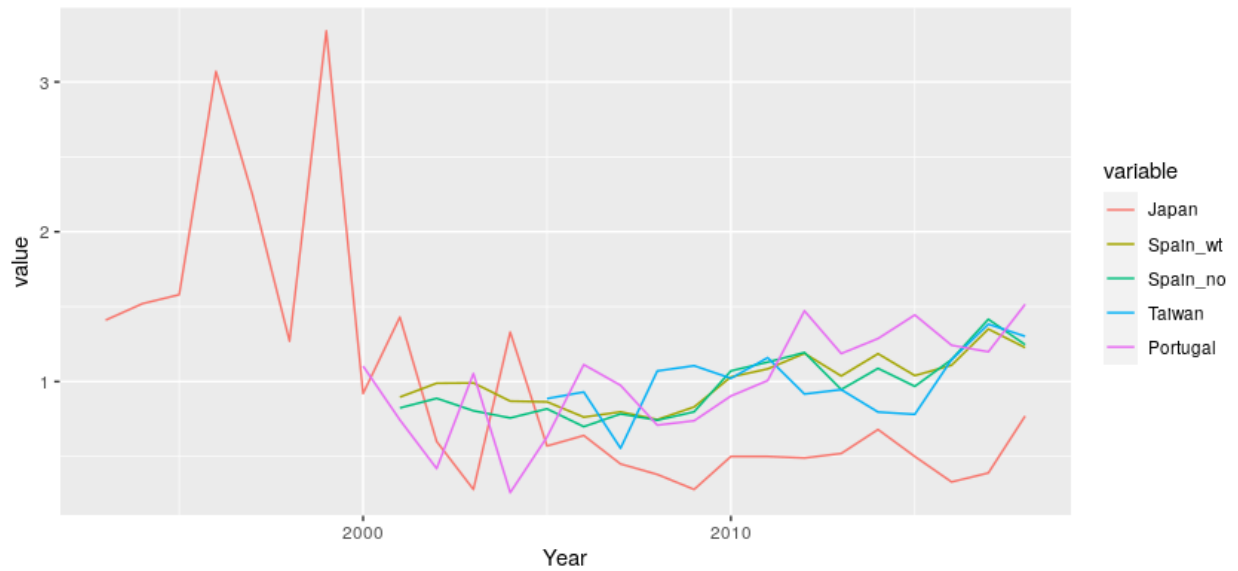
Figure 6. The standardised CPUE indices as reported to the IOTC by Japan, EU,Spain, Taiwan,China and EU,Portugal that have been scaled by dividing by the mean of each index.

Table 2. The CPUE indices used in this study were run in the models as both the standardised CPUEs given by Japan, EU,Portugal, EU,Spain and Taiwan,China, and with a scaling performed. The scaling was performed with the 'scale' function in the R base package, with centers 0.2607692 for Japan, 53.6043889 for EU,Spain, 0.1775957 for Taiwan,China, and 102.8 for EU,Portugal.

Year	Standardised				Scaled			
	Japan	Spain	Taiwan	Portugal	Japan	Spain	Taiwan	Portugal
1993	1.41				1.41			

Year								
1994	1.52				1.52			
1995	1.58				1.58			
1996	3.07				3.07			
1997	2.24				2.24			
1998	1.27				1.27			
1999	3.34				3.34			
2000	0.92			113.4	0.92			1.10311284
2001	1.43	48.059		76.5	1.43	0.8965497228		0.7441634241
2002	0.6	53.018		43.1	0.6	0.9890608045		0.4192607004
2003	0.28	53.119		108.3	0.28	0.9909449786		1.053501946
2004	1.33	46.598		26.6	1.33	0.8692944918		0.2587548638
2005	0.57	46.346	0.1574	64.7	0.57	0.8645933842	0.8862826484	0.6293774319
2006	0.64	40.886	0.1652	114.4	0.64	0.7627360529	0.9302026272	1.112840467
2007	0.45	42.769	0.09857	100.2	0.45	0.7978637736	0.5550246547	0.9747081712
2008	0.38	40.017	0.19018	72.9	0.38	0.7465246938	1.070859175	0.7091439689
2009	0.28	44.52	0.19636	75.9	0.28	0.8305290093	1.105657312	0.7383268482
2010	0.5	55.253	0.18141	92.9	0.5	1.030755152	1.021477352	0.9036964981
2011	0.5	58.132	0.2059	103.5	0.5	1.08446344	1.159374824	1.006809339
2012	0.49	63.68	0.16283	151.3	0.49	1.187962428	0.9168577105	1.471789883
2013	0.52	55.595	0.168	122	0.52	1.037135226	0.9459687734	1.186770428
2014	0.68	63.566	0.14144	132.3	0.68	1.185835737	0.7964156149	1.286964981
2015	0.5	55.745	0.13875	148.5	0.5	1.039933505	0.781268853	1.444552529
2016	0.33	59.449	0.20355	127.7	0.33	1.109032324	1.146142523	1.242217899
2017	0.39	72.388	0.24557	123.2	0.39	1.350411813	1.382747331	1.19844358
2018	0.77	65.739	0.23118	155.8	0.77	1.226373462	1.301720601	1.515564202

4. Setting priors by method

Following the CMSY best practice guide ([Froese et al. 2015](#)), and based on our best knowledge of biological information, we define different priors for multiple runs of each of the methods. The results of these runs will be compared to establish the best case for the different methods.

4.1 CMSY

A full list of the CMSY parameters are outlined in Table 3. When setting CMSY priors, the CMSY guidelines (Froese et al. 2015) recommend searching for the information in previous assessments if available (even if the assessment is derived from other ocean basins), FishBase, or by visualising the catch and CPUE data (see Table 1 for recommendations on where to find information for each prior).

Table 3. The CMSY parameters and their description. The default values assigned by CMSY are identified and an example of values for Run 5 (see Table 6) using SMA data of this analysis are given.

CMSY parameter name	Description	CMSY default values	SMA example Run 5
MinOfYear	the start year of the catch report	First year of dataset	1964
MaxOfYear	the end year of the catch report	Last year of dataset	2018
r.low	an optional parameter to specify the range of intrinsic growth rate for the species.		0.0081
r.hi	as above		0.0484
startb.low	the prior biomass range relative to the unexploited biomass (B/k) at the beginning of the catch time series (Table 5)	0.2	0.4
startb.hi	as above	0.6	0.9
intb.yr	a year in the time series for an intermediate biomass level. Set it to NA to have it estimated by default rules.	Automatically calculated at 10 years prior to the end of the time series	2000
intb.low	the estimated intermediate relative biomass range (see Table 5). Set it to NA to have it estimated from maximum or minimum catch, according to some simple rules (note: these may not be appropriate for your stock).	0.2	0.1
intb.hi	as above	0.6	0.9
endb.low	the prior relative biomass (B/k) range at the end of the catch time series (see next section). Set to NA if you want to use the defaults	0.01	0.2
endb.hi	as above	0.4	0.7
q.start	the start and end year for determining the catchability coefficient. Set to a recent period of at least 5 years where catch and abundance were relatively stable or had similar trends. If set to NA the default is last 5 years (or last 10 years in slow growing species).	5 years prior to the end of the catch time series	2000
q.end	as above	Last year of the catch time series	2018
StartYear	Start year for catch time series	First year auto-read from dataset	1964
EndYear	End year for catch time series	Penultimate year auto-read from dataset	2018
Blim	optional; fisheries reference points from assessments, for comparison, not used in the analysis	NA	NA
Bpa	as above	NA	NA

BMSY	as above	NA	NA
B40	as above	NA	NA
FMSY	as above	NA	NA
Flim	as above	NA	NA
FPA	as above	NA	NA
Fofl	as above	NA	NA
last_F	as above	NA	NA
MSY	as above	NA	NA
SSBMSY	as above	NA	NA
btype	the type of information in the bt column of the catch file. Allowed values are "biomass" (when total biomass is reported), "CPUE" (when cpue or cpue index or SSB are reported) or "None" (if no abundance data are available)	None	None
force.cmsy	check if the management analysis should use the CMSY results rather than available BSM results. Useful when the abundance data are deemed unreliable. Default is FALSE or F.		TRUE

4.1.1 Catch time series requirements

For CMSY, it is important that the catch time series represents the full range of catch variability of the fishery, including high and low periods, and be at least 15 years long. While noting this, many species have catch time series that include years of poor data quality, e.g., before sampling was routine. CMSY guidelines note that CMSY should be run starting when the catch time series is considered reliable (StartYear). This reliability can be derived from expert opinion.

In the case of the SMA, Brunel et al. 2018 use reconstructed catch data based on swordfish and and tuna catch time series beginning in 1971, as this is the year when many shark stock assessment models begin, and is before the expansion in the 1970s of oceanic fisheries in the Indian Ocean (Coehlo and Rosa, 2017). The nominal catch data of SMA from the IOTC begins in 1964 (Figure 4), and shows a wide variability in catch over its length, including high catch in the beginning of the dataset, which decreases in the 1970s and then increases again in the 1990s (Figure 4). The number of observations increases from 1986 onwards as SMA begins to be reported by a variety of different fisheries and CPCs (Figure 4).

For this study, we examine the effect of time series start year, including catch time series starting in 1964 or 1971 (Table 6).

4.1.2 Resilience, or intrinsic growth rate, *r*

The intrinsic growth rate, r, or the 'resilience' strongly influences the results of the model. This value, ranging from >0 to 1, represents the ability of the population to regenerate, and depends on the life history of the species. Species that grow quickly with fast growth and short generation times generally have higher values of r than species with slow growth and long generation times (Table 5 gives qualitative and quantitative ranges of r).

Brunel et al. (2018) derived their range of r by developing a demographic analysis via a stochastic population dynamics model based on Leslie Matrices. They investigated uncertainty in the biological characteristics of SMA (see Biological information). They found that when assuming a reproductive cycle of 2 years (0.032 - 0.0484), r tended to be higher than compared to when they assumed a generation time of 3 years (0.0081 and 0.025). Thus, Brunel et al. 2018 tested a range of r between their lowest and highest estimates, i.e. 0.00081 to 0.0484. Our demographic analysis indicates an r of about 0.016. This falls into the range tested by Brunel et al. 2018. Both estimates correspond to the "Very low" range of the qualitative CMSY parameter and reflects what we know of SMA, that they are a slow-growing, late-maturing species that produce relatively few offspring.

Fishbase indicates that the r for SMA is 0.24 with 95% CI of 0.11 to 0.54, corresponding to a "Low" to "Medium" range of r values (Table 5). Considering what we know of the biology of SMA and Brunel et al.'s analysis, the FishBase r estimate appears too high.

As r is such an influential variable, we find it valuable to estimate ourselves, and have developed a demographic analysis based on Leslie Matrices, similar to Brunel et al (2018), with the r estimated as 0.031 and CV = 0.2 (see details in Section 4.2.1). This value is consistent with the range tested by Brunel; thus we set the prior r range to between 0.0081 and 0.0484 (Table 6).

Table 5. Quantitative ranges of qualitative categories of intrinsic growth rate, or resilience, r, and the depletion rate, or biomass relative to the unfished stock, B/k.

Resilience / intrinsic growth rate	prior r range
High	0.6 – 1.5
Medium	0.2 – 0.8
Low	0.05 – 0.5
Very low	0.015 – 0.1
Depletion rate	**prior relative biomass (B/k) range**
Very strong depletion	0.01 – 0.2
Strong depletion	0.01 – 0.4
Medium depletion	0.2 – 0.6
Low depletion	0.4 – 0.8

Nearly unexploited	0.75 – 1.0

4.1.3 Depletion, biomass relative to unfished stock

Depletion ranges between 0.01 and 1. Stocks that have never been fished can have a value of 1, though otherwise, the value must be <1. Likewise, stocks with reasonable catches must have a depletion rate of >0.01. Froese et al. 2015 note that the width of the relative biomass ranges should be at least 0.4, unless the stock is known to be strongly depleted, in which case they suggest ranges of e.g., 0.01-0.3 or 0.01-0.2. Table 5, summarised from the guidelines, gives the general range of depletion rate values of stocks under very strong depletion to nearly unexploited.

4.1.3.1 Starting depletion range

Brunel et al. (2018) estimate that SMA was lightly fished by 1971 when their assessment starts, and they used a starting depletion range (startb.low, startb.hi) of between 0.7 to 0.9, which Froese et al. 2015 indicate to be in the 'Nearly unexploited' range (Table 5). We note that the full nominal catch time series (Figure 4) indicates more catch prior to 1971 than after 1971; thus we set a wider range of depletion, from 0.4 to 0.9.

4.1.3.2 Intermediate depletion range

The guidelines note that the analysis is improved if the intermediate depletion range (intb.low, intb.hi, intb.yr) is set to the last year of either the highest or lowest biomass, with a correspondingly high or low biomass range. For example, if the last highest biomass was in 2004, then set int.yr to 2004, and the biomass range to e.g., 0.4 to 0.8. If an intermediate depletion range is not specified, the default set by the CMSY algorithm is 0.2 to 0.6 set 10 years before the final year of the time series. Brunel et al. 2018 found this range too restrictive, and thus set a wider range between 0.1 to 0.9 fifteen years prior to the end of their time series (i.e. 2000).

Similarly, here, we set a wider range between 0.1 and 0.9 starting in 2000, as in Brunel et al. 2018.

4.1.3.3 Ending depletion range

The default ending depletion range is quite low (0.01 to 0.4). Brunel et al. (2018) gave a wide depletion rate range for the ending depletion (endb.low, endb.hi) for the last year in their analysis (2015) so as not to restrict the model, i.e. between 0.2 and 0.7. We follow their example for our analysis.

4.1.4 Catchability

The remaining parameters considered by the CMSY method involve estimates of catchability (q.start, q.end). The method determines catchability within a period of at least 5 years where catch was relatively stable or had similar trends. If no time period is set for this prior, the method will investigate the last 5

years of the dataset, or the last 10 years for a slow growing species. Based on the catch data ([Figure 4](#)), we note that catch is highly variable over the last 20 years. Furthermore, we note that a catchability that is representative of the full time series will have more stable results. Thus, we set the range of years over which to estimate the catchability between 2000 and 2018, which also includes the majority of the CPUE data ([Table 2](#)).

4.1.5 Biomass type

In CMSY, the user must specify the type of index, which can be "biomass", "CPUE", or "none" in the case where no abundance index is available. Here, we specify "CPUE" when testing the different CPUE indices and "none" when we test only catch data.

A complete list of the prior values for each run are given in [Table 6](#).

Table 6. The priors that are tested using the CMSY method (n=10 runs).

Run	CPUE	Start Year	End Year	r.low	r.hi	stb. low	stb. hi	intb. yr	intb. low	intb. hi	endb. low	endb .hi	q. start	q. end	btype	force. cmsy
1	SMAIOTC_scaled CPUE_JPN	1971	2018	0.0081	0.0484	0.4	0.9	2000	0.1	0.9	0.2	0.7	2000	2018	CPUE	F
2	SMAIOTC_scaled CPUE_SPN	1971	2018	0.0081	0.0484	0.4	0.9	2000	0.1	0.9	0.2	0.7	2000	2018	CPUE	F
3	SMAIOTC_scaled CPUE_TWN	1971	2018	0.0081	0.0484	0.4	0.9	2000	0.1	0.9	0.2	0.7	2000	2018	CPUE	F
4	SMAIOTC_scaled CPUE_POR	1971	2018	0.0081	0.0484	0.4	0.9	2000	0.1	0.9	0.2	0.7	2000	2018	CPUE	F
5	SMAIOTC	1964	2018	0.0081	0.0484	0.4	0.9	2000	0.1	0.9	0.2	0.7	2000	2018	None	T
6	SMAIOTC	1971	2018	0.0081	0.0484	0.4	0.9	2000	0.1	0.9	0.2	0.7	2000	2018	None	T
7	SMAIOTC_scaled CPUE_JPN	1964	2018	0.0081	0.0484	0.4	0.9	2000	0.1	0.9	0.2	0.7	2000	2018	CPUE	F
8	SMAIOTC_scaled CPUE_SPN	1964	2018	0.0081	0.0484	0.4	0.9	2000	0.1	0.9	0.2	0.7	2000	2018	CPUE	F
9	SMAIOTC_scaled CPUE_TWN	1964	2018	0.0081	0.0484	0.4	0.9	2000	0.1	0.9	0.2	0.7	2000	2018	CPUE	F
10	SMAIOTC_scaled CPUE_POR	1964	2018	0.0081	0.0484	0.4	0.9	2000	0.1	0.9	0.2	0.7	2000	2018	CPUE	F

4.2 JABBA

JABBA offers the possibility to define prior information of the intrinsic growth rate of the population *r* and the unfished equilibrium biomass *K*.

4.2.1 Prior on the intrinsic growth rate of the population r

We used a Leslie population model to compute the population growth rate. We followed Mangel & Broziak (2010) and Simon et al. (2012) to estimate *r* from biological parameters. This classical approach has been widely used in ecology and is one of the demographic methods reviewed by Stobberup & Erzini (2006) to elucidate the prior of the population growth rate. The population is described by *N(t)* vector of length *A* describing the number of individuals in each age-class at time *t*, with terminal age *A* (number of age groups). A transition matrix *T* determines the contribution of each individual to the next age-group and to the new generation. The entries of the Leslie matrix are *S(i)* and *F(i)*: i.e., the survival rate from age *i* to age *i+1* and the fecundity at age *i* (i.e. the average number of age zero female individuals produced by an individual), respectively. In the matrix form, the model is written in the recurrence relationship (1):

$$[N_i]_{t+1} = T.[N_i]_t \qquad (1)$$

As T coefficients are all positive and constant over time, the composition of the population at t+n can be predicted by (2):

$$[N_i]_{t+n} = T^n.[N_i] \qquad (2)$$

As t tends to infinity, the system reaches equilibrium and the contribution of each age group in the total population becomes stable. The population growth rate, *r*, is *r = ln(λ)* with *λ* being the dominant eigenvalue of matrix *T.* In our Monte Carlo approach, *r* is computed for 10,000 Leslie population matrices resulting from 10,000 random realizations in the pdf parameters.

The survival rate is estimated from $S(i) = e^{-M(i)}$ where $M_{(i)}$ is the natural mortality at age *i*. As natural mortality at age is very different between early life stages and older ages, we split the calculation of M in these two periods.

4.2.1.1 Natural mortality for early life stages

The *in utero* mortality is estimated from McGurk (1986) relationship:

$$M_0 = \sum_{t=1}^{365} a_{young}.W_{t,Young}^{b_{young}} \qquad (3)$$

where a_{young} and b_{young} are parameters estimated by McGurk (1986) with values of 0.00022 and -0.85 respectively and $W_{t, Young}$ is the dry weight of the animal in g at day *t*. We use a ratio of 0.15 to convert weight in dry weight as suggested in Kamler (1992). We sum over the first 365 days although pup age can be up to 18 months. The estimation of the mortality rate after age 1 with this method is very similar to

the one that will be described after. We therefore preferred to estimate the mortality after 1 year using the other methods.

The weight of the young was derived from Mollet et al. (2000) weight-length relationship:

$$a_{wYoung} * L_{Young}{}^{bwYoung} \quad (4)$$

where a_{wYoung} and b_{wYoung} are parameters estimated by Mollet et al. (2000) with values of 8.198 and 3.117 respectively and L_{Young} is the length of the pups in cm.

The growth of pups in utero was defined as a Gompertz curve such as:

$$L_{Young} = L_{infYoung}.e^{(-k1*exp(-k2*t))} \quad (5)$$

where $L_{infYoung}$ is the theoretical maximum length of the pup size in utero in cm, $k1$ and $k2$ are two parameters of the Gompertz equation which defines the growth rate and inflexion time of the growth.

4.2.1.2 Natural mortality for juveniles and adults

Three methods are compared to estimate the natural mortality for juveniles and adults.
Then et al. (2015) propose an age-independent natural mortality using the equation:

$$M = 4.899.MaxAge^{-0.916} \quad (6)$$

Chen and Watanabe (1989) equation is described as:

$$M_{mat} = \sum_{t=1}^{A_{mat}} k/(1-e^{(-k.(t-t0))}) \quad (7)$$

Where k and t_0 are the von Bertalanffy growth curve coefficients and, A_{mat} is the age at maturity

$$M_{adult} = \sum_{t=A_{mat}+1}^{MaxAge} k/[a_0 + a_1*((t-A_{mat}) + a_2*(t-A_{mat})^2] \quad (8)$$

with $a_0 = 1-e^{[-k.(Amat-t0)]}$, $a_1 = k*e^{[-k*(Tmat-t0)]}$, and $a_2 = -0.5*k^{2*exp[-k*(Amat-t0)]}$

McGurk (1986) confirmed Peterson & Wroblewski (1984) equation:

$$M = \sum_{t=366}^{365*MaxAge} 0.00526.W_t{}^{-0.25} \quad (9)$$

where W_t is the dry weight (in gram) of the individual at age t (in day). The weight is calculated from the weight-length relationship:

$$W_{adult} = a_{adult}. L_{adult}{}^{badult} \quad (10)$$

And L_{adult} is calculated from the von Bertalanffy growth curve:

$$L_{adult} = L_{inf} . (1-e^{-k.(t-t0)}) \quad (11)$$

Where L_{inf}, k and t_0 are the three parameters of the von Bertalanffy model.

4.2.1.3 Fecundity

The fecundity of shortfin mako shark is estimated from Mollet et al. (2000) equation:

$$LS = 0.810.L_i^{2.346} \quad (12)$$

where LS is the litter size, and L_i is the length in cm at age i. We assume a sex ratio of 1:1 to derive the number of female offspring.

4.2.1.4 Monte carlo simulation for r

For the different biological parameters, we assume a distribution over the best estimates from the literature. When a range of values for a given parameter was available, a uniform distribution with 10,000 sampling is chosen. In other cases, we multiply the best estimate value by a random number with a normal distribution with a mean of 1 and a standard deviation of 0.1.

Table 7. Parameters used for estimating r.

Parameter	Best estimate or range	Reference
a_{young}	0.00022	McGurk (1986)
b_{young}	-0.85	McGurk (1986)
a_{WYoung}	8.198	Mollet et al (2000)
b_{WYoung}	3.117	Mollet et al (2000)
$L_{infYoung}$	73 cm	Mollet et al (2000)
Linf	350.3	Rosa et al. (2017)
k	0.064	Rosa et al. (2017)
t_0	-3.09 years	Rosa et al. (2017)
MaxAge	29-32 years	Natanson et al. (2006)
A_{mat}	18-21 years	Mollet et al (2000)
a_{adult}	0.0000052432	IOTC conversion factor
b_{adult}	3.1407	IOTC conversion factor

4.2.2 Prior estimates of unfished equilibrium biomass K

For the unfished equilibrium biomass K, the default settings of the JABBA R package were applied, which is a vaguely informative lognormal prior with a large CV of 100% and a central value that corresponds to eight times the maximum total catch, which is consistent with parameterization procedures followed when using other platforms such as Catch-MSY (Martell and Froese, 2013) or SPiCt (Pedersen and Berg 2017). All catchability parameters were formulated as uninformative uniform priors, while additional observation variances were estimated for each index by assuming inverse-gamma priors to enable model internal variance weighting. Here, the process error of log(By) in year y was estimated "freely" by the model using an uninformative inverse-gamma distribution with both scaling parameters setting at 0.001.

4.2.3 Surplus biomass models

Regarding the surplus biomass model, we used the four available options in JABBA: Fox, Schaefer, Pella-Tomlinson model and the Pella-Tomlinson hockey-stick composite model.

The 28 different scenarios are described in Table Scenarios:

Table Scenarios: Combinations of model types and CPUE time series used that resulted in the 28 scenarios

Scenario	Model type	CPUE used
1	Schaefer	JPN+TWN+EU.Spain+EU.Port
2	Fox	JPN+TWN+EU.Spain+EU.Port
3	Pella-Tomlinson	JPN+TWN+EU.Spain+EU.Port
4	Pella-Tomlinson composite	JPN+TWN+EU.Spain+EU.Port
5	Schaefer	JPN
6	Fox	JPN
7	Pella-Tomlinson	JPN
8	Pella-Tomlinson composite	JPN
9	Schaefer	TWN
10	Fox	TWN

11	Pella-Tomlinson	TWN
12	Pella-Tomlinson composite	TWN
13	Schaefer	EU.Spain
14	Fox	EU.Spain
15	Pella-Tomlinson	EU.Spain
16	Pella-Tomlinson composite	EU.Spain
17	Schaefer	EU.Port
18	Fox	EU.Port
19	Pella-Tomlinson	EU.Port
20	Pella-Tomlinson composite	EU.Port
21	Schaefer	TWN+EU.Spain+EU.Port
22	Fox	TWN+EU.Spain+EU.Port
23	Pella-Tomlinson	TWN+EU.Spain+EU.Port
24	Pella-Tomlinson composite	TWN+EU.Spain+EU.Port
25	Schaefer	JPN+TWN+EU.Spain
26	Fox	JPN+TWN+EU.Spain
27	Pella-Tomlinson	JPN+TWN+EU.Spain
28	Pella-Tomlinson composite	JPN+TWN+EU.Spain

5 Stock assessment results and discussion

5.1 Prior on the intrinsic population growth rate

The natural mortality-at-age estimated by the three different methods give similar results (Figure 7).
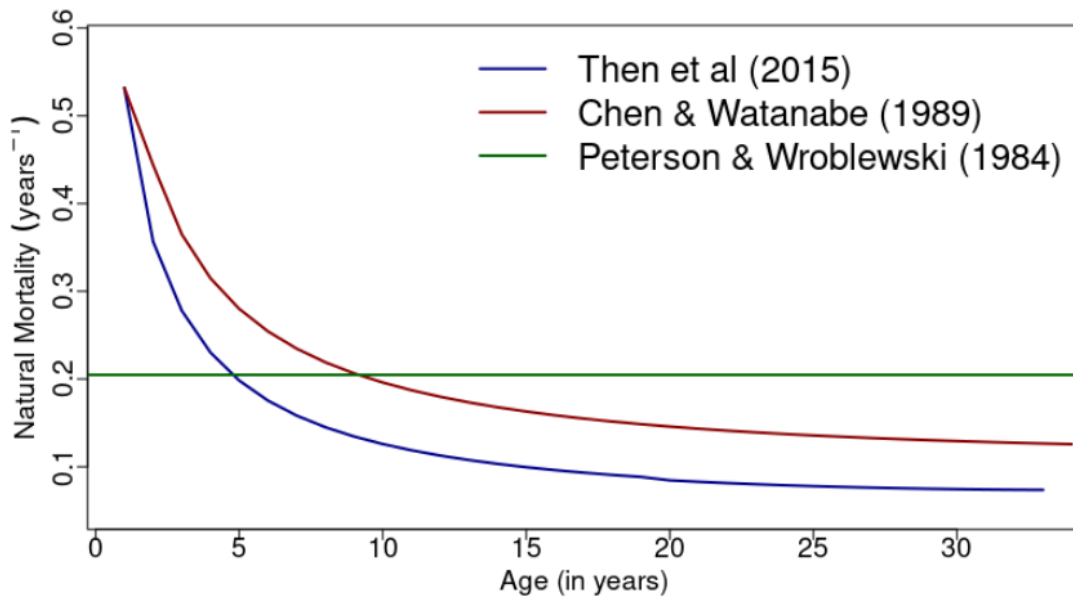
Figure 7: Estimates for the natural mortality at age for three different methods

Ten thousand bootstraps of the different combinations of biological parameters gave a distribution for *r* for these three methods to estimate the natural mortality (Figure 8).
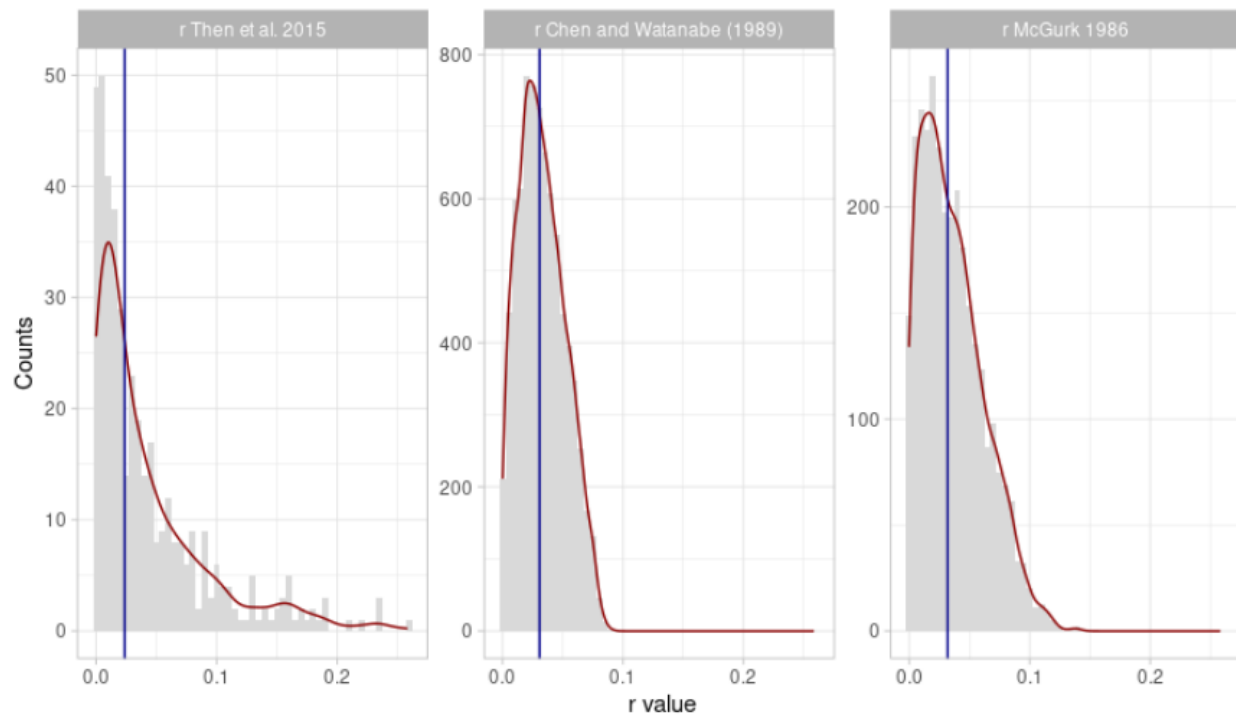

Figure 8: Distribution of the estimate for *r* for the 10 000 bootstraps in the biological parameter distribution and three different methods to estimate the natural mortality. Note that the negative values have been excluded.

The values for *r* are very similar for the three methods with median values of 0.02367 using Then et al (2015), 0.03063 using Chen & Watanabe (1989), and 0.03194 using McGurk (1986).

The prior value used for *r* with JABBA will be 0.031 with a CV of 0.2.

5.2 CMSY and BSM

5.2.1 Effect of the starting year of the catch time series

When running CMSY (Run 5 and 6: catch-only, no CPUE index included, Table 6), setting the start year to 1964 or 1971 had no effect on the *r*. The *K* increased slightly with the longer time series from 181.32 kt to 186.10 kt (Figure 9).

Figure 9. The r-K pairs found by CMSY when using the full catch time series from 1964 (left panel), and when using the catch time series from 1971 as in Brunel et al. 2018 (right panel). The dark grey points relate to the r-k pairs found by the CMSY model to be compatible with the catches and prior information. The blue cross indicates the most probable r-k pair and the approximate 95% confidence limits.

Likewise, we find that the start year of the catch time series has minimal impact on the results of the different runs when including CPUE. The runs that include the Japan CPUE are different from the runs using other CPUE indices (e.g. in their K, Bmsy, Fmsy; Table 8), but the runs with the Japan CPUE examined across different start years have similar results. This lack of influence in start year is likely because the catch rate of the catch data prior to 1971 is lower than the current catch rate (Figure 6), and therefore has little impact on the estimates of K.

Table 8. A summary of the results from CMSY (catch-only) and the BSM runs including CPUE indices from Japan (JPN), EU,Spain (SPN), Taiwan,China (TWN), EU,Portugal (POR).

Run	CPUE	start. yr	end. yr	msy	r	k	msy	B	Bmsy	B. Bmsy	F	Fmsy	F. Fmsy

1	JPN	1971	2018	1.010	0.017	243.305	1.010	65.326	121.653	0.537	0.026	0.008	3.122
2	SPN	1971	2018	0.982	0.020	192.035	0.982	113.681	96.017	1.184	0.015	0.010	1.456
3	TWN	1971	2018	0.916	0.020	183.117	0.916	101.952	91.559	1.114	0.017	0.010	1.660
4	POR	1971	2018	0.948	0.020	189.958	0.948	105.912	94.979	1.115	0.016	0.010	1.602
5	Catch-only	1964	2018	1.404	0.031	181.321	1.404	97.376	90.660	1.074	0.017	0.015	1.123
6	Catch-only	1971	2018	1.441	0.031	186.101	1.441	100.169	93.050	1.077	0.017	0.015	1.092
7	JPN	1964	2018	1.027	0.017	246.706	1.027	65.177	123.353	0.528	0.026	0.008	3.119
8	SPN	1964	2018	0.973	0.021	185.325	0.973	115.672	92.663	1.248	0.015	0.011	1.393
9	TWN	1964	2018	0.927	0.021	179.770	0.927	102.158	89.885	1.137	0.017	0.010	1.607
10	POR	1964	2018	0.943	0.020	186.479	0.943	105.162	93.240	1.128	0.016	0.010	1.591

Thus, our final model configuration includes a start year from 1964, so as to consider the full dataset available.

5.2.2 Effect of the CPUE indices

The CPUE index from Japan gives a lower r and a higher K than the other CPUE indices tested. The Japan CPUE shows much higher values in the early years of the index, descending in value in the more recent years (Figure 6). The opposite pattern is observed for the other three indices. Due to this early period of high CPUE, the initial biomass (K) is estimated at a higher level, which then impacts the estimation of both Bmsy and Fmsy. We find that the other three indices tested show similar results across their r, K, Bmsy and Fmsy (Table 8).

Comparing between the results of the CMSY (catch-only) runs and those using the BSM (Table 8), we find that CMSY estimates a higher r (0.031) relative to the BSM results (0.017-0.021) (Figure 10, panel C).
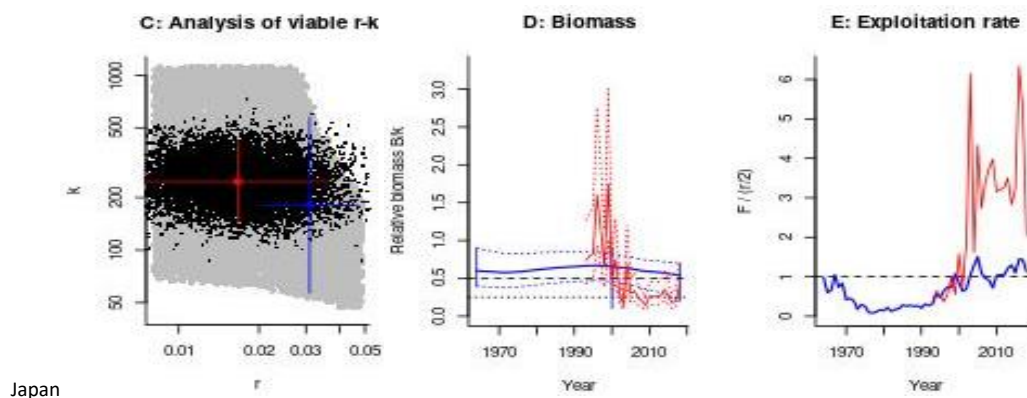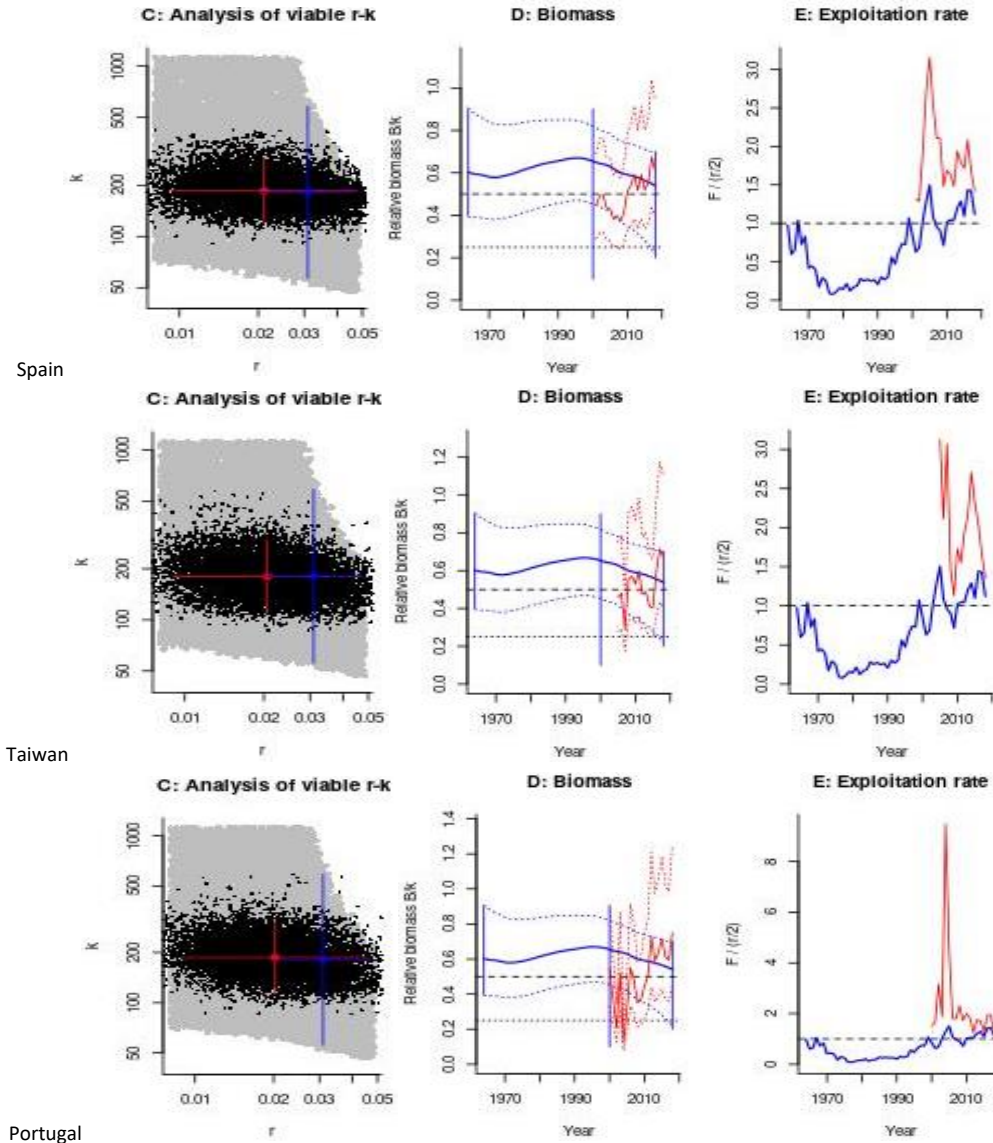
Figure 10. Output of the Bayesian Schaefer model using the CPUE indices from (top to bottom) Japan, EU,Spain, Taiwan,China and EU,Portugal. Panel C shows the r/K pairs found by CMSY catch-only and BSM when using the full catch time series with the dark grey points indicating possible r-k pairs found by CMSY that are compatible with the catch data and prior information. The blue cross indicates the most probable r-k pair and the 95% confidence interval as found by the CMSY (catch-only). The black dots are possible r-k pairs found by the BSM model, with a red cross indicating the most probable r-k pair and its 95% confidence limits. Panel D shows the estimated biomass relative to K (red), i.e., the CPUE data, scaled to the BSM estimate of Bmsy = 0.5 k, and in blue the biomass trajectory estimated by CMSY. Dotted blue lines indicate the 2.5th and 97.5th percentiles. Vertical blue lines indicate the prior biomass ranges. Horizontal dashed and dotted black lines indicates the 0.5 and 0.25 biomass, respectively. Panel E indicates the exploitation rate (catch/abundance) scaled to the r/2 estimated from the BSM (red) and from the CMSY (blue). The black horizontal dotted line indicates where F/Fmsy = 1.

The Japan and Portugal BSMs indicate that biomass was low around 2000 (Figure 10). For the Japan BSM, it remains low until 2018, but the Portugal BSM shows that it increases by 2018. Spain and Taiwan BSMs

do not indicate the earlier decline, and they show increasing biomass by 2018. The CMSY (catch only) biomass estimate is in more agreement with the Japan BSM than the other BSMs, and indicates decreasing biomass from 2000 to 2018 (Figure 10, panel D). However, the B/Bmsy estimated by the CMSY (catch only) are more in line with the BSMs from Spain, Taiwan, and Portugal with B/Bmsy > 1, indicating that the stock is not overfished (Table 8). In contrast, the Japan BSM estimates that B/Bmsy = 0.53, indicating that the stock is overfished.

All BSMs and the CMSY (catch-only) outputs indicate that the stock is undergoing overfishing (F/Fmsy > 1) (Table 8). The BSMs indicate that overfishing has been occurring almost entirely from the start of when abundance indices are available, and the CMSY indicate overfishing in the last 15 years. CMSY outputs indicate that exploitation rates begin relatively high and decline and stabilise in the 1970s and 1980s. They increased from the 1990s and reached overfishing levels by 2000. Exploitation appears to decline again near 2010, and then increase to overfishing again by the end of the time series (Figure 10, panel E).

Examining the stock trajectories produced by the different runs, we find that all runs except for BSM Japan indicate that the stock is in the 'orange' (top-right quadrant of Figure 11). In contrast, BSM Japan indicates that the stock is in the 'red' (top-left quadrant of Figure 11).
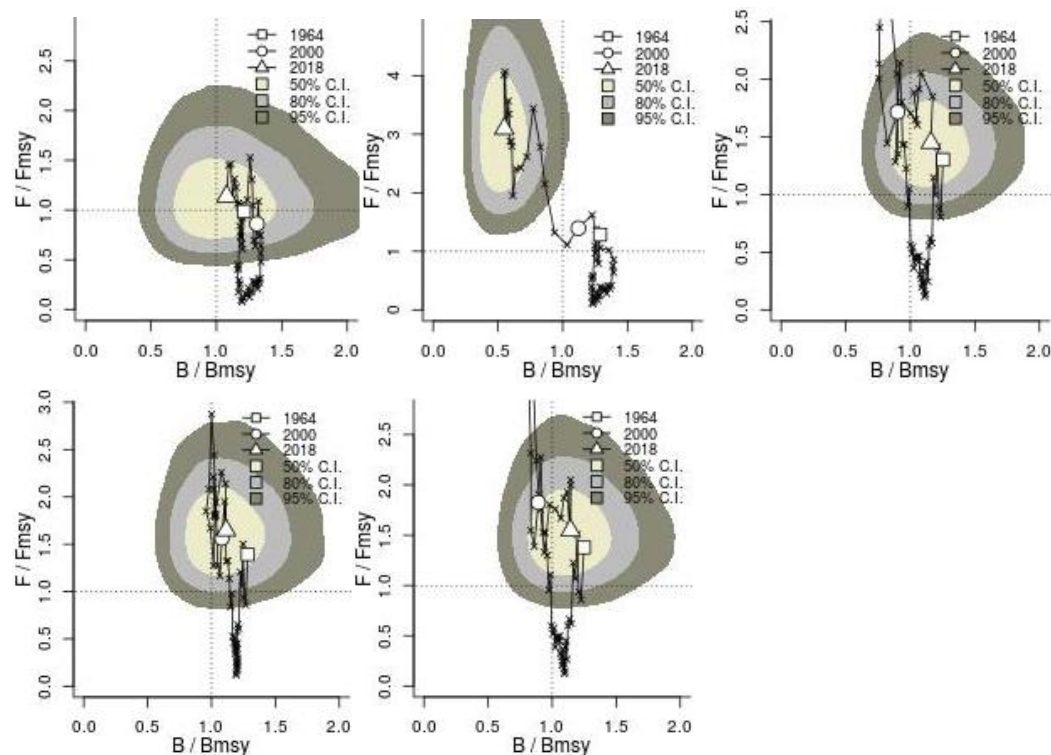
Figure 11. The trajectory of relative stock size (B/Bmsy) over relative exploitation (F/Fmsy) for CMSY catch only Run 5 (top left), BSM Japan (top middle), BSM Spain (top right), BSM Taiwan (bottom left), and BSM Portugal (bottom right). These plots are similar to Kobe plots, but quadrants are not colored and must be inferred, i.e. red (top-left), orange (top-right), yellow (bottom-left), green (bottom-right).

5.3 JABBA

Twenty-eight different runs have been performed resulting from a combination of
-   four different model types (Fox, Schaefer, Pella & Tomlinson, and Pella & Tomlinson hockey-stick composite model); and
-   the inclusion of a combination of the four different CPUE time series , i.e. a jackknife analysis.

The comparison of the outputs of key values (K, B_{MSY}, F_{MSY}, MSY, r, B/B_{MSY}, F/F_{MSY}) shows two clear patterns: (i) the inclusion of the Japanese CPUE leads to more pessimistic stock status and (ii) the Schaefer model is, as expected, the most conservative model (Figure 12).
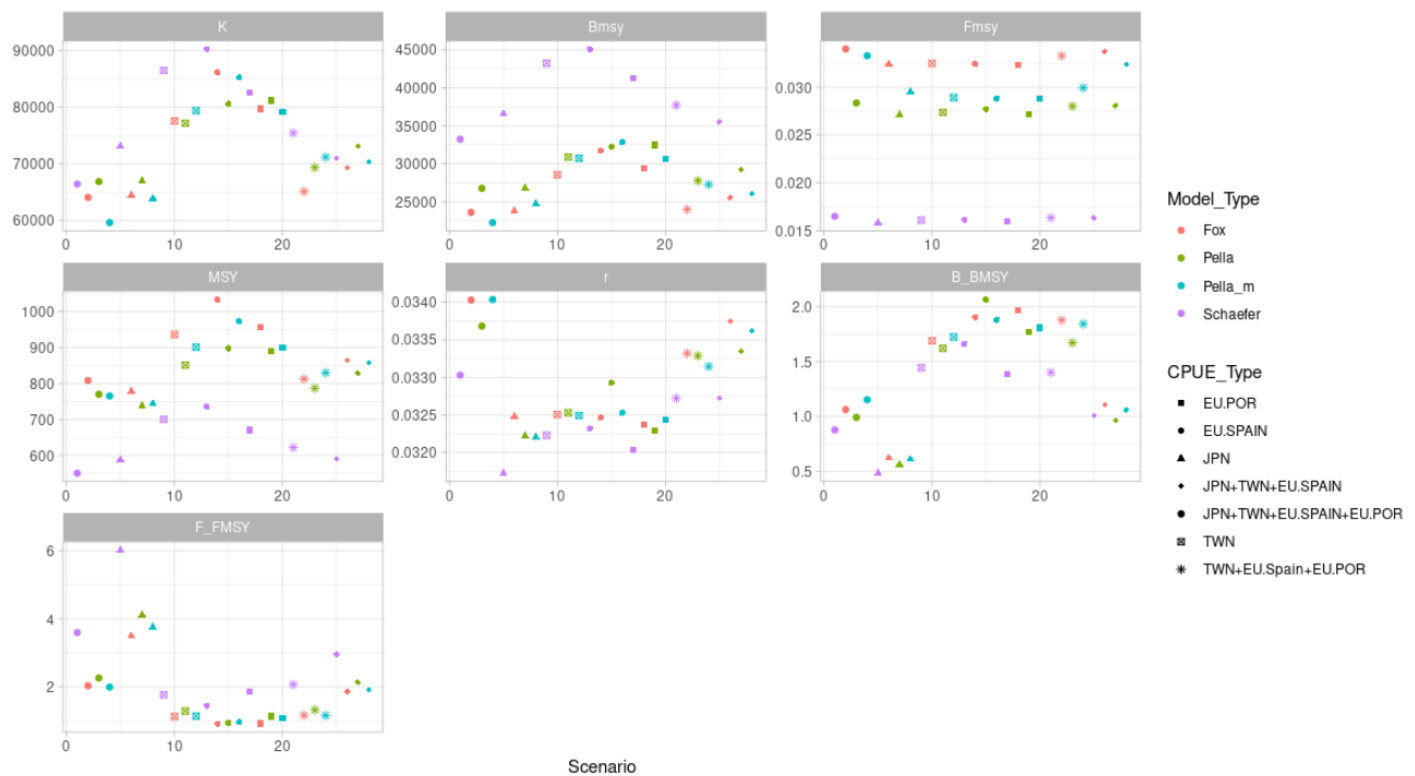
Figure 12. Values for different key outputs from stock assessment (K, B_{MSY}, F_{MSY}, MSY, r, B/B_{MSY}, F/F_{MSY}) resulting from the different combinations of model type used and CPUE time series included in the stock assessment.

Depending on the value of the shape parameter *m*, the Pella & Tomlinson model converges towards a Fox model when *m* tends to 1 and a Schaefer model when *m* equals 2. The selection of Pella & Tomlinson model seems a reasonable option as the shape parameter gives more flexibility in the surplus production curve - the drawback being to overfit the data. A first run with all CPUE shows that the Japanese CPUE strongly deviates in the early period of the time series (Figures 13 and 14). In the different simulations, it shows that values from the Pella-Tomlinson models are within the range of values between the Fox and the Schaefer model (Figure 12).

The removal of the Japanese CPUE time series improved the quality of the fit to the CPUE (Figure 15). The comparison of the two runs (with or without the Japanese CPUE) indicate the stock status is more pessimistic with the Japanese CPUE than without it (Figure 16).

We find the comparison of the Mohn's rho between the retrospective pattern of these two runs show that the run without the Japanese CPUE is more stable (Table 9). Some values for rho for the run with the Japanese CPUE are outside the acceptable range of -0.15 and 0.20 (Hurtado-Ferro et al. 2014; Carvalho et al. 2017). This may be because of the conflicting trends between the Japanese CPUE (overall decreasing abundance) compared to the other CPUE indices (overall increasing abundance), which the model has difficulty in handling (Figure 6).

However, when comparing the hindcasting cross-validation results for these two runs, we find that the run with all CPUEs shows that the Japanese CPUE has a low mean absolute scaled error (MASE), indicating a good ability to predict future values abundance while the MASE are higher for the other CPUE (Figure 17). This may be due to its long time series.

The different figures and tables for these two runs are available in Appendix 2.
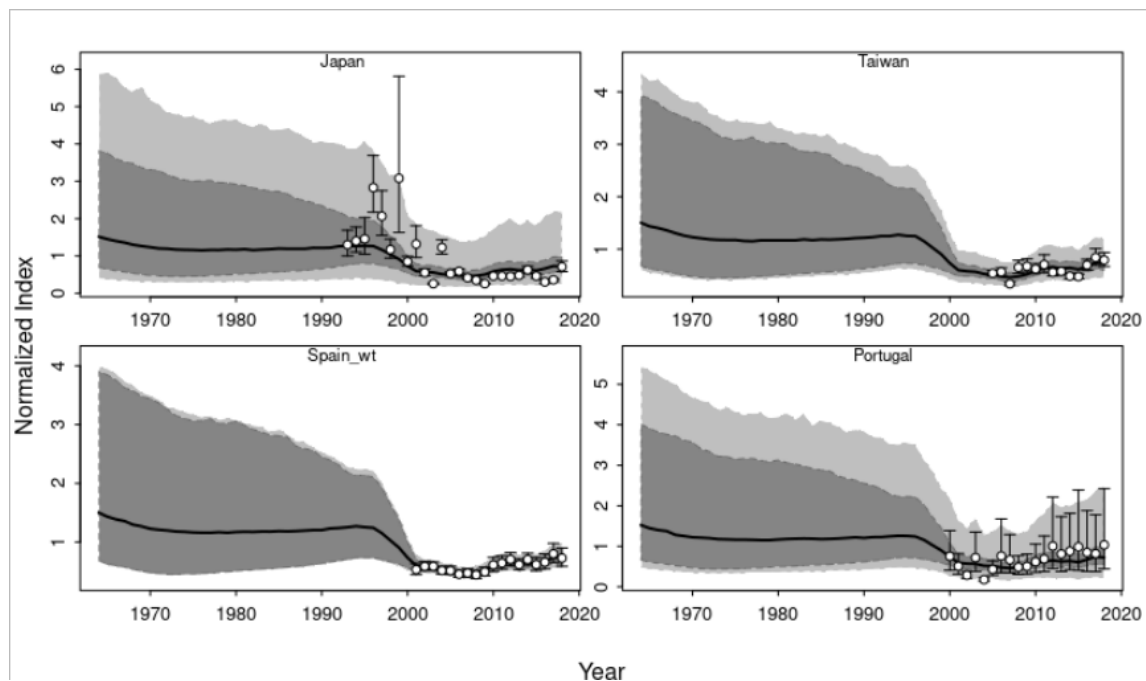
Figure 13: Time-series of observed (circle) with error 95% CIs (error bars) and predicted (solid line) CPUE of Indian Ocean shortfin mako for the Bayesian state-space surplus production model JABBA. The dark shaded grey areas show 95% credibility intervals of the expected mean CPUE and the light shaded grey areas denote the 95% posterior predictive distribution intervals.
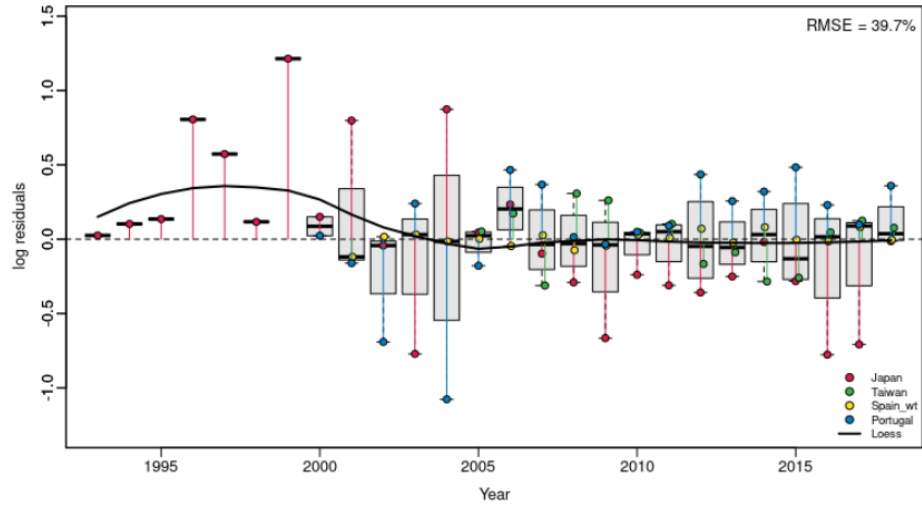
Figure 14: JABBA residual diagnostic plots of CPUE indices including all the available time series, i.e boxplots indicating the median and quantiles of all residuals available for any given year, and solid black lines indicate a loess smoother through all residuals.
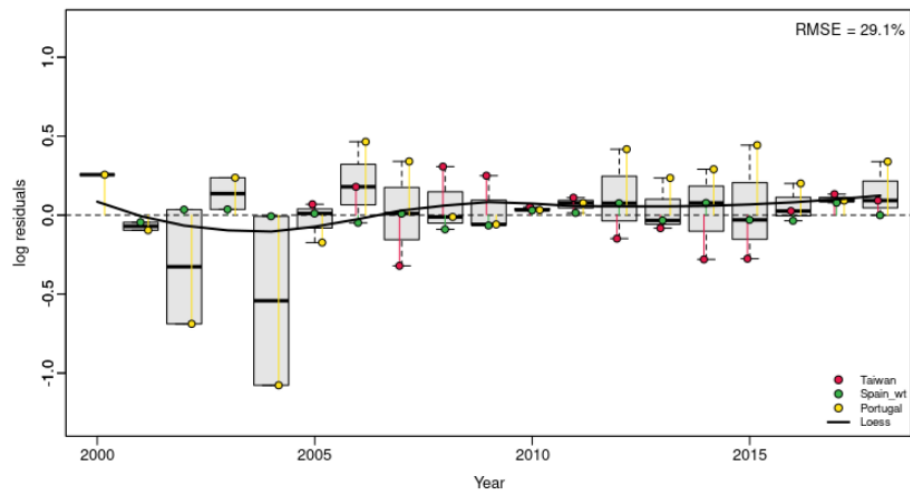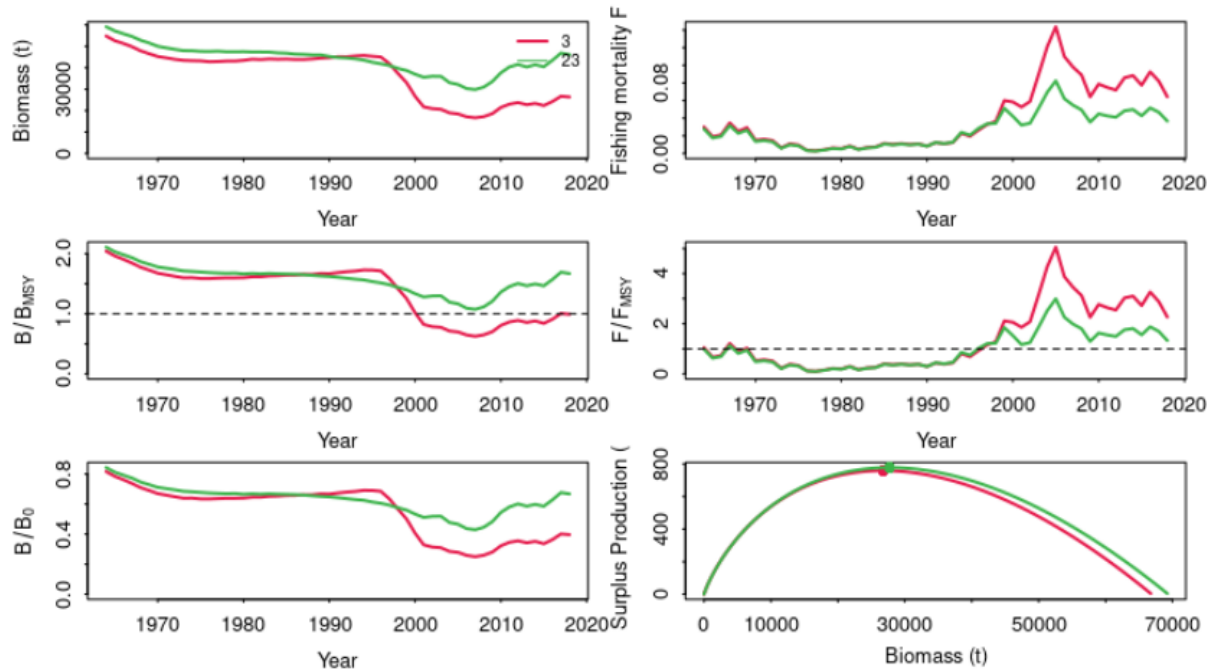

Figure 15: JABBA residual diagnostic plots of CPUE indices including all the available time series but the Japanese CPUE, i.e boxplots indicating the median and quantiles of all residuals available for any given year, and solid black lines indicate a loess smoother through all residuals.

Figure 16: Comparison of the main stock assessment outputs between the run with all CPUE included (run 3, red line) and the run without the Japanese CPUE (run 23, green line).

Table 9: Comparison of the Mohn's rho calculated from the retrospective analyses for the run with or without the Japanese CPUE.

Model runs	B	F	B_{MSY}	F_{MSY}	B/B_0	MSY
Run 3 (all CPUEs)	-0.2547	0.3567	-0.1564	0.3497	-0.1564	-0.1140
Run 23 (without Japanese CPUE)	-0.0452	0.0529	0.0131	0.0499	0.01310	-0.0804
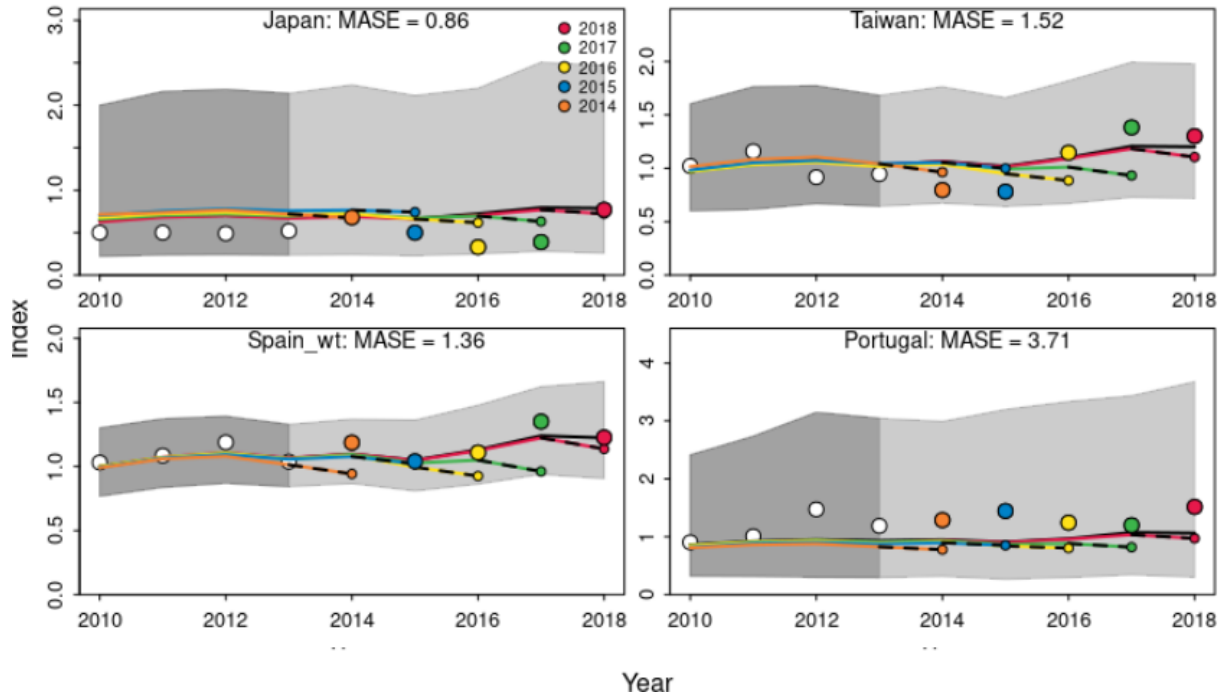
Figure 17: Hindcasting cross-validation results (HCxval) for the run with all CPUE include showing one-year-ahead forecasts of CPUE values (2010-2018), performed with 5 hindcast model runs relative to the expected CPUE. The CPUE observations, used for cross-validation, are highlighted as colored solid circles with associated light-grey shaded 95% confidence interval. The model reference year refers to the end points of each one-year-ahead forecast and the corresponding observation (i.e. year of peel + 1).

A summary of posterior quantiles for parameters and management quantities of interest for the two runs of the JABBA model are presented in Table 10 with the comparison for the 2 runs. Depending on the selected run by the WPEB group, the executive summary will be provided with related data and figures.

Table 10: Summary of posterior quantiles presented in the form of marginal posterior medians and associated the 95% credibility intervals of parameters for the JABBA Model with all CPUEs included or without the Japanese CPUE.

Run	Parameter Estimated	Median	LCI (2.5%)	UCI (97.5%)
All CPUE	K	66879	33711	181988
Without JPN CPUE	K	69361	37145	140777
All CPUE	r	0.03368	0.02270	0.05048
Without JPN CPUE	r	0.03328	0.02220	0.04975
All CPUE	F_{MSY}	0.1167	0.03277	0.2007

Without JPN CPUE	F_{MSY}	0.1162	0.03242	0.2000
All CPUE	B_{MSY}	13375	669	26081
Without JPN CPUE	B_{MSY}	13871	693	27049
All CPUE	F/F_{MSY}	2.2665	1.0673	2.2665
Without JPN CPUE	F/F_{MSY}	1.3295	0.5610	3.0001
All CPUE	B/B_{MSY}	0.99155	0.4074	1.8776
Without JPN CPUE	B/B_{MSY}	1.669	0.7282	2.8134
All CPUE	MSY	385	19	750
Without JPN CPUE	MSY	393	20	767

5.4 Comparison between methods

We find high consistency between the CMSY catch-only and BSM runs with CPUE indices in their estimates of r, K, Fmsy, Bmsy, F/Fmsy, B/Bmsy and MSY (Table 8). The exception is the BSM Japan, which gives more pessimistic outcomes.

Similarly, JABBA results indicate that the Japan CPUE significantly alters the results of the model, with more pessimistic results when it is included. We find that the Japanese CPUE has a conflicting trend to the other CPUEs, leading to less stable model diagnostics when it is included. However, retrospective analyses indicate the Japanese CPUE index itself appears more stable than the others, with a good ability to predict.

Our methods show similar results to the Brunel et al (2018) preliminary stock assessments. Their models indicated overfishing from the mid 1990s (F/Fmsy = 2.57). In terms of F/Fmsy, the CMSY runs are lower in magnitude than Brunel et al.'s (i.e. between 1.1 to 1.25, though BSM Japan F/Fmsy = 3.1), but they also all indicate overfishing. Both JABBA runs indicate overfishing as well, with the run without JPN CPUE lower in magnitude (1.33) than the all CPUE run (2.27).

Brunel et al (2018) show decreasing biomass, which is not overfished (B/Bmsy close to 1). Likewise, CMSY runs indicate B/Bmsy close to 1, except for the BSM Japan, which indicates that the stock is overfished (B/Bmsy=0.54). JABBA runs show a decrease in biomass from the mid-1960s to the late 2000s and an upward trend afterward. For the run with all CPUEs included, the stock has equal chances to be overfished or not overfished. For the run without the Japanese CPUE, the stock is not overfished in 92% of bootstraps.

Thus, we note that both CMSY and JABBA give results that are generally consistent with the past assessment (i.e. Brunel et al. 2018), but we also note that the inclusion of the Japanese CPUE significantly

alters the results. We therefore suggest that the group decide on the best case scenario as either the JABBA All CPUE run or the JABBA run without Japanese CPUE.

References

Barreto, R.R., de Farias, W.K.T., Andrade, H., Santana, F.M., Lessa, R. 2016. Age, Growth and Spatial Distribution of the Life Stages of the Shortfin Mako, Isurus oxyrinchus (Rafinesque, 1810) Caught in the Western and Central Atlantic. PLoS ONE 11(4): e0153062.

Bishop, S. & Francis, Malcolm & Duffy, Clinton & Montgomery, John. (2006). Age, growth, maturity, longevity and natural mortality of the shortfin mako shark (Isurus oxyrinchus) in New Zealand waters. Marine and freshwater research. 57. 143-154. 10.1071/MF05077.

Brunel T., Coelho R., Merino G., Ortiz de Urbina J., Rosa D., Santos C, Murua H., Bach P., Saber S., Macias D.. 2018. A Preliminary Stock Assessment for the Shortfin Mako Shark in the Indian Ocean using Data-limited Approaches. IOTC-WPEB14-2018-037.

Cailliet, G.M., Cavanagh, R.D., Kulka, D.W., Stevens, J.D., Soldo, A., Clo, S., Macias, D., Baum, J., Kohin, S., Duarte, A., Holtzhausen, J.A., Acuña, E., Amorim, A. & Domingo, A. 2009. Isurus oxyrinchus (Atlantic subpopulation). The IUCN Red List of Threatened Species 2009: e.T161749A5494807. https://dx.doi.org/10.2305/IUCN.UK.2009-2.RLTS.T161749A5494807.en.

Carvalho F, A.E. Punt, Y.J. Chang, M.N. Maunder, K.R. Piner 2017. Can diagnostic tests help identify model misspecification in integrated stock assessments? Fish. Res., 192 (2017), pp. 28-40, 10.1016/j.fishres.2016.09.018

Casey, J.G. and Kohler, N.E. 1992. Tagging studies on the shortfin mako shark (Isurus oxyrinchus) in the western North Atlantic. Australian Journal of Marine and Freshwater Research 43: 45-60.
Cliff, G., Dudley, S.F.J. and Davis, B. 1990. Sharks caught in the protective gillnets of Natal, South Africa. 3. The shortfin mako shark Isurus oxyrinchus (Rafinesque). South African Journal of Marine Science 9: 115-126.

Cliff, G., Dudley, S.F.J. and Davis, B. 1990. Sharks caught in the protective gillnets of Natal, South Africa. 3. The shortfin mako shark Isurus oxyrinchus (Rafinesque). South African Journal of Marine Science 9: 115-126.

Coelho R. Rosa D. 2017. Catch Reconstruction For The Indian Ocean Blue Shark: An Alternative Hypothesis Based On Ratios. IOTC-2017-WPEB13-22.

Coelho R., Santos C, Rosa D. 2020. Updated Fishery Indicators for Shortfin Mako Shark (Isurus oxyrinchus) Caught by the Portuguese Pelagic Longline Fishery in the Indian Ocean: Catch, Effort And Standardized Cpues. IOTC–2020–WPEB16–15.

Compagno, L.J.V. 2001. Sharks of the world. An annotated and illustrated catalogue of shark species known to date. Volume 2. Bullhead, Mackerel and Carpet Sharks (Heterodontiformes, Lamniformes and Orectolobiformes). FAO, Rome.

Csirke, J. and Sharp, G.D. 1984. Proceedings of the Expert Consultation to examine changes in abundance and species of neritic fish resources. San José, Costa Rica. 18-29/04/1983. FAO Fisheries Report, 291 (2) : 553 p.

Fishbase. Isurus oxyrinchus Rafinesque, 1810: Shortfin mako. https://www.fishbase.se/summary/752. Accessed 4 August 2020.

Francis, M.P. And Duffy, C. 2005. Length at maturity in three pelagic sharks (Lamna nasus, Isurus oxyrinchus, and Prionace glauca) from New Zealand. Fishery Bulletin 103: 489-500.

Froese R., Demirel N., Coro G., Kleisner K.M., Winker, H. (2017) Estimating Fisheries Reference Points from Catch and Resilience. Fish and Fisheries, 18: 506-526 DOI: 10.1111/faf.12190.

Froese R., Demirel N., Coro G., and Winker H. 2019. A Simple User Guide for CMSY+ and BSM (CMSY_2019_9f.R). Published online at http://oceanrep.geomar.de/33076/ in December 2019. Accessed 5 August 2020.

Groeneveld J. C., Cliff G., Dudley S. F. J., Foulis A. J., Santos J., and Wintner S. P. 2014. Population structure and biology of shortfin mako, Isurus oxyrinchus, in the south-west Indian Ocean. CSIRO Marine and Freshwater Research. http://dx.doi.org/10.1071/MF13341.

Holts, D.B. and Kohin, S. 2003. Pop-up archival tagging of shortfin mako sharks, Isurus oxyrinchus, in the Southern California Bight. Anstract. American Fisheries Society, Western Division meetings. American Fisheries Society, San Diego, California.

Hurtado-Ferro F, Cody S. Szuwalski, Juan L. Valero, Sean C. Anderson, Curry J. Cunningham, Kelli F. Johnson, Roberto Licandeo, Carey R. McGilliard, Cole C. Monnahan, Melissa L. Muradian, Kotaro Ono, Katyana A. Vert-Pre, Athol R. Whitten, André E. Punt, Looking in the rear-view mirror: bias and retrospective patterns in integrated, age-structured stock assessment models, ICES Journal of Marine Science, Volume 72, Issue 1, January 2015, Pages 99–110, https://doi.org/10.1093/icesjms/fsu198.

Imzilen T, Bonhommeau S, Rouyer T, Kell LT, Chassot E, Barde J 2016. Online collaborative environment to run Stock Assessment work ow: an option for IOTC? IOTC-2016-WPM-13 Rev_1.

IOTC 2016. Shortfin mako shark : Supporting Information. https://iotc.org/sites/default/files/documents/science/species_summaries/english/Shortfin%20mako%20shark%20Supporting%20Information.pdf.

Kai M., Semba Y. 2019. Estimation of Annual Catch Rates and Catches for Shortfin Mako (Isurus oxyrinchus) Caught By Japanese Longline Fishery Operated in the Indian Ocean from 1993 to 2018. IOTC-2019-WPEB15-21.

Kamler, E. (1992). Characteristics of fish reproductive products. In Early Life History of Fish (pp. 31-106). Springer, Dordrecht.

Klimley, A.P., Beavers, S.C., Curtis, T.H. and Jorgensen, S.J. 2002. Movements and swimming behavior of three species of sharks in La Jolla Canyon, California. Environmental Biology of Fishes 63: 117-135.

Li, B., Ouyang, W., Sheng, L., Zeng, X., Wang, X. 2019. GS3D: An Efficient 3D Object Detection Framework for Autonomous Driving. https://arxiv.org/abs/1903.10955. Accessed 27 August 2020.

Mangel M, Brodziak J, DiNardo G (2010) Reproductive ecology and scientific inference of steepness: a fundamental metric of population dynamics and strategic fisheries management. Fish and Fisheries 11: 89–104.

Martell S, Froese R 2013. A simple method for estimating MSY from catch and resilience. Fish and Fisheries 14(4). doi: 10.1111/j.1467-2979.2012.00485.x

McGurk MD (1986) Natural mortality of marine pelagic fish eggs and larvae: role of spatial patchiness. Mar Ecol Prog Ser 34: 227–242.

Mejuto J, García-Cortés B, Ramos-Cartelle A (2006) An Overview Of Research Activities On Swordfish (Xiphias Gladius) And The By-catch Species, Caught By The Spanish Longline Fleet In The Indian Ocean. IOTC 2006-WPB-11.

Mildenberger TK, Taylor MH, Wolff M (2017). "TropFishR: an R package for fisheries analysis with length-frequency data." Methods in Ecology and Evolution, 8(11), 1520–1527. ISSN 2041-210X, doi: 10.1111/2041-210X.12791, http://dx.doi.org/10.1111/2041-210X.12791.

Mildenberger, T. 2020. Length-frequency data for TropFishR. https://cran.r-project.org/web/packages/TropFishR/vignettes/lfqData.html. Accessed on 8 August 2020.

Mildenberger, T. 2020. Single-species fish stock assessment with TropFishR. https://cran.r-project.org/web/packages/TropFishR/vignettes/tutorial.html. Accessed on 5 August 2020.

Mollet, H.F., Cliff, G., Pratt, H.L., Jr. and Stevens, J.D. 2000. Reproductive biology of the female shortfin mako Isurus oxyrinchus Rafinesque 1810, with comments on the embryonic development of lamnoids. Fishery Bulletin 98(2): 299-318.

Murua H, Coelho, R., Santos, M.N., Arrizabalaga, H., Yokawa, K., Romanov, E., Zhu, J.F., Kim, Z.G., Back, P., Chavance, P., Delgado de Molina and Ruiz, J. (2012). Preliminary Ecological Risk Assessment (ERA) for shark species caught in fisheries managed by the Indian Ocean Tuna Commission (IOTC). IOTC–2012–SC15–INF10 Rev_1.

Murua, H., Abascal, F.J., Amande, J., Ariz, J., Bach, P., Chavance, P., Coelho, R., Korta, M., Poisson, F., Santos, M.N., Seret, B. 2013a. EUPOA-Sharks: Provision of scientific advice for the purpose of the implementation of the EUPOA sharks. Studies for Carrying out the Common Fisheries Policy; Reference: MARE/2010/11Final Report. European Commission. 443 pp.

Natanson , L.J., Kohler, N.E., Ardizzone, D., Cailliet, G.M., Wintner, S.P. and Mollet, H.F. 2006. Validated age and growth estimates for the shortfin mako, Isurus oxyrinchus, in the North Atlantic Ocean. Environmental Biology of Fishes 77: 367-383.

Nieblas A-E, Bonhommeau S, Imzilen T, Fu D, Fiorellato F, Barde J (2017). An online tool to easily run stock assessment models, using SS3 and YFT as an example. IOTC-2017-WPM08-12Rev_1. In: IOTC Proceedings. Victoria, Seychelles, 13-15 October 2017, 24p.

Pedersen, M. W. and Berg, C. W. 2017. A stochastic surplus production model in continuous time. Fish and Fisheries. 18:226-243.

Peterson, I., & Wroblewski, J. S. (1984). Mortality rate of fishes in the pelagic ecosystem. Canadian Journal of Fisheries and Aquatic Sciences, 41(7), 1117-1120.

Pratt, H.L. and Casey, J.G. 1983. Age and growth of the shortfin mako, Isurus oxyrinchus. In: In: Prince, E.D. and Pulos, L.M. (eds). (eds), Proceedings of the international workshop on age determination of oceanic pelagic fishes: Tunas, billfishes, and sharks NOAA Tech. Rep. NMFS 8: 175-177.

Ramos-Cartelle, A, Fernández-Costa, J., and Mejuto J. 2020. Standardized Catch Rates of Shortfin Mako (Isurus oxyrinchus) Caught by the Spanish Surface Longline Fishery Targeting Swordfish in the Indian Ocean during the Period 2001-2018. IOTC-2020-WPEB16-16

Rosa, D., Mas, F., Alyssa, M., Natanson, L.J., Domingo, A., Carlson, J., Coelho, R. 2017. Age and growth of shortfin mako in the North Atlantic, with revised parameters for consideration to use in the stock assessment. 2017 ICCAT Shortfin mako assessment meeting, 12-16 June 2017, Madrid, Spain. ICCAT document SCRS/2017/111: 22 pp.

Sepulveda, C.A., Kohin, S., Chan, C., Vetter, R. and Graham, J.B. 2004. Movement patterns, depth preferences, and stomach temperatures of free-swimming juvenile mako sharks, Isurus oxyrinchus, in the Southern California Bight. Marine Biology 145(1): 191-199.

Schwamborn, R., Mildenberger, T., and Taylor, M. 2018. Assessing sources of uncertainty in length-based estimates of body growth in populations of fishes and macroinvertebrates with bootstrapped ELEFAN. Ecological Modelling. 393. 10.1016/j.ecolmodel.2018.12.001.

Simon, M., Fromentin, J. M., Bonhommeau, S., Gaertner, D., Brodziak, J., & Etienne, M. P. (2012). Effects of stochasticity in early life history on steepness and population growth rate estimates: An illustration on Atlantic bluefin tuna. PloS one, 7(10), e48583.

Smith, S.E., Au, D.W. and Show, C. 1998. Intrinsic rebound potentials of 26 species of Pacific sharks. Marine and Freshwater Research 49(7): 663-678.

Sparre, P., and SC Venema. 1998. "Introduction to Tropical Fish Stock Assessment." FAO Technical Paper.

Stevens, J.D. 1983. Observations on reproduction in the shortfin mako Isurus oxyrinchus. Copeia 1983(1): 126-130.

Stobberup KA, Erzini K (2006) Assessing mackerel scad, Decapterus macarellus, in Cape Verde: Using a Bayesian approach to biomass dynamic modelling in a data-limited situation. Fisheries Research 82: 194–203 doi:10.1016/j.fishres.2006.06.005.

Taylor, M.H. 2020. Using the TropFishR ELEFAN functions. https://cran.r-project.org/web/packages/TropFishR/vignettes/Using_TropFishR_ELEFAN_functions.html. Accessed on 5 August 2020.

Tsai W.-P., Wu X.-H., Liu K.-M. 2019. Standardized CPUE of Shortfin Mako Sharks by the Taiwanese Large-scale Tuna Longline Fishery in the Indian Ocean. IOTC-2019-WPEB15-22.

Winker, H., Carvalho, F., Kapur, M. (2018) JABBA: Just Another Bayesian Biomass Assessment. Fisheries Research 204: 275-288.

Appendix 1. Catch per unit effort (CPUE) as provided by Japan, EU,Spain, EU,Portugal, and Taiwan,China.

A1.1 CPUE Japan

Taken from Table 5 of IOTC-2019-WPEB15-21.

Year	Nominal CPUE	Standardised CPUE	Scaled standardised CPUE	Estimated catch weight (tons)	Estimated catch number	Total landings (number)	Total landing (number) for filtered data	Total number of hooks (one millions)	Coefficient of variations	Lower value (scaled CPUE) 95% CI	Upper value (scaled CPUE) 95% CI
1993	0.63	0.37	1.41	487	12356	4322	2849	39.6	0.095	1.19	1.73
1994	0.64	0.4	1.52	1768	31516	7136	4175	72.2	0.079	1.33	1.81
1995	0.31	0.41	1.58	1965	36330	5623	2731	87.7	0.107	1.29	1.95
1996	1.16	0.8	3.07	5217	100623	13487	10557	104.7	0.044	2.84	3.38
1997	0.61	0.58	2.24	3593	93034	11555	7629	118.5	0.065	1.98	2.55
1998	0.19	0.33	1.27	2358	38990	4691	1768	111.5	0.086	1.11	1.56
1999	0.51	0.87	3.34	5082	76290	6180	2871	98.1	0.097	2.87	4.12
2000	0.32	0.24	0.92	983	15546	5697	2306	95.3	0.085	0.81	1.13
2001	0.17	0.37	1.43	1260	23279	4232	1569	104.7	0.113	1.18	1.84
2002	0.1	0.16	0.6	893	13431	3100	590	95.6	0.139	0.49	0.81
2003	0.05	0.07	0.28	333	4811	1725	169	72.3	0.137	0.22	0.38
2004	0.34	0.35	1.33	1702	31647	5598	2336	91.9	0.059	1.19	1.49
2005	0.15	0.15	0.57	1150	20675	4985	1271	104.7	0.068	0.51	0.67
2006	0.13	0.17	0.64	1203	20292	3720	1221	107.2	0.081	0.55	0.75
2007	0.1	0.12	0.45	647	11109	2808	806	98.1	0.104	0.37	0.55
2008	0.14	0.1	0.38	403	7466	5357	3897	82.4	0.084	0.33	0.46
2009	0.12	0.07	0.28	229	4062	4707	3495	66.1	0.055	0.26	0.32
2010	0.17	0.13	0.5	328	5352	4473	3550	40.2	0.06	0.44	0.56
2011	0.2	0.13	0.5	184	3712	4876	4143	32.1	0.074	0.44	0.59
2012	0.15	0.13	0.49	256	4576	3648	2926	34.1	0.054	0.44	0.55
2013	0.17	0.13	0.52	261	4233	3002	2327	32	0.091	0.43	0.61
2014	0.14	0.18	0.68	379	6178	2531	1918	33	0.105	0.56	0.84

2015	0.14	0.13	0.5	250	3894	2255	1619	29.9	0.122	0.39	0.63
2016	0.12	0.09	0.33	161	2607	1816	957	27.7	0.255	0.19	0.52
2017	0.1	0.1	0.39	189	2706	1646	1020	24.2	0.113	0.31	0.49
2018	0.14	0.2	0.77	285	4256	1682	1033	22.5	0.134	0.57	0.96

A1.2 CPUE (weight) EU,Spain

Caption and table taken from Table 3 of IOTC-2020-WPEB16-16: Estimated parameters (lsmean), standard error (stderr), standardized CPUE in weight (CPUEw) of shortfin mako and upper and lower 95% confidence limits for the Spanish longline fleet in the Indian Ocean during the period analyzed 2001-2018.

YEAR	LSMEAN	STDERR	UCPUEw	CPUEw	LCPUEw
2001	3.8684	0.0898	57.307	48.059	40.304
2002	3.9686	0.064	60.105	53.018	46.766
2003	3.9707	0.06	59.75	53.119	47.223
2004	3.8396	0.0622	52.64	46.598	41.249
2005	3.8337	0.07	53.165	46.346	40.401
2006	3.7091	0.0584	45.845	40.886	36.464
2007	3.7532	0.0718	49.231	42.769	37.154
2008	3.6864	0.0756	46.407	40.017	34.506
2009	3.7931	0.0757	51.64	44.52	38.382
2010	4.0073	0.0961	66.698	55.253	45.772
2011	4.0589	0.088	69.071	58.132	48.926
2012	4.1508	0.0789	74.333	63.68	54.554
2013	4.0154	0.0731	64.158	55.595	48.175
2014	4.1495	0.0722	73.227	63.566	55.181
2015	4.0166	0.0913	66.664	55.745	46.614
2016	4.0804	0.097	71.897	59.449	49.156
2017	4.277	0.101	88.231	72.388	59.391
2018	4.1799	0.1075	81.154	65.739	53.253

A1.3 CPUE EU,Portugal

Caption and table taken from Table 3 of IOTC-2020-WPEB16-15: Standardized SMA CPUE index (kg/1000 hooks) for the Portuguese pelagic longline fleet in the Indian Ocean between 2000 and 2018, for use as a relative biomass index indicator. The table includes the standardized CPUE index value, the 95% confidence intervals (CI) and the coefficient of variation (CV, %).

Year	Stdz CPUE (Kg/1000 hks)	Upper CI (95%)	Lower CI (95%)	CV (%)
2000	113.4	132	97.5	28.2
2001	76.5	85.9	68	32.9
2002	43.1	49.3	37.8	37.8
2003	108.3	121.3	96.6	30.5
2004	26.6	32.4	21.8	42.6
2005	64.7	82.7	50.6	32.9
2006	114.4	123.4	106	36.2
2007	100.2	109.1	92	34.6
2008	72.9	88.1	60.4	32.7
2009	75.9	86.5	66.5	32.4
2010	92.9	105.4	81.9	30.2
2011	103.5	115.3	92.9	30.5
2012	151.3	168.5	135.9	27.4
2013	122	132.2	112.6	32.6
2014	132.3	144.4	121.3	28.7
2015	148.5	160.4	137.5	31.2
2016	127.7	137.9	118.3	32.7
2017	123.2	133.3	113.9	33
2018	155.8	170.2	142.6	28.6

A1.4 CPUE Taiwan,China

Caption and table taken from Table 3: IOTC-2019-WPEB15-22: Estimated nominal and standardized CPUE values for shortfin mako shark of the Taiwanese tuna longline fishery in the Indian Ocean.

Year	Nominal	Standardised	Lower CI	Upper CI
2005	0.04718	0.1574	0.06075	0.25405
2006	0.04911	0.1652	0.04038	0.29002
2007	0.02899	0.09857	0.00573	0.19142
2008	0.06137	0.19018	0.00197	0.3784
2009	0.06186	0.19636	0.00665	0.38608
2010	0.05684	0.18141	0.03184	0.33098
2011	0.06973	0.2059	-0.03042	0.44221
2012	0.05712	0.16283	0.03641	0.28925
2013	0.05021	0.168	0.04172	0.29429
2014	0.04306	0.14144	0.03612	0.24675
2015	0.04359	0.13875	0.04895	0.22855
2016	0.06404	0.20355	0.05633	0.35076
2017	0.07968	0.24557	0.06255	0.4286
2018	0.07302	0.23118	0.06372	0.39865

Appendix 2: Outputs from the Run 3 (Pella & Tomlinson with all CPUEs)
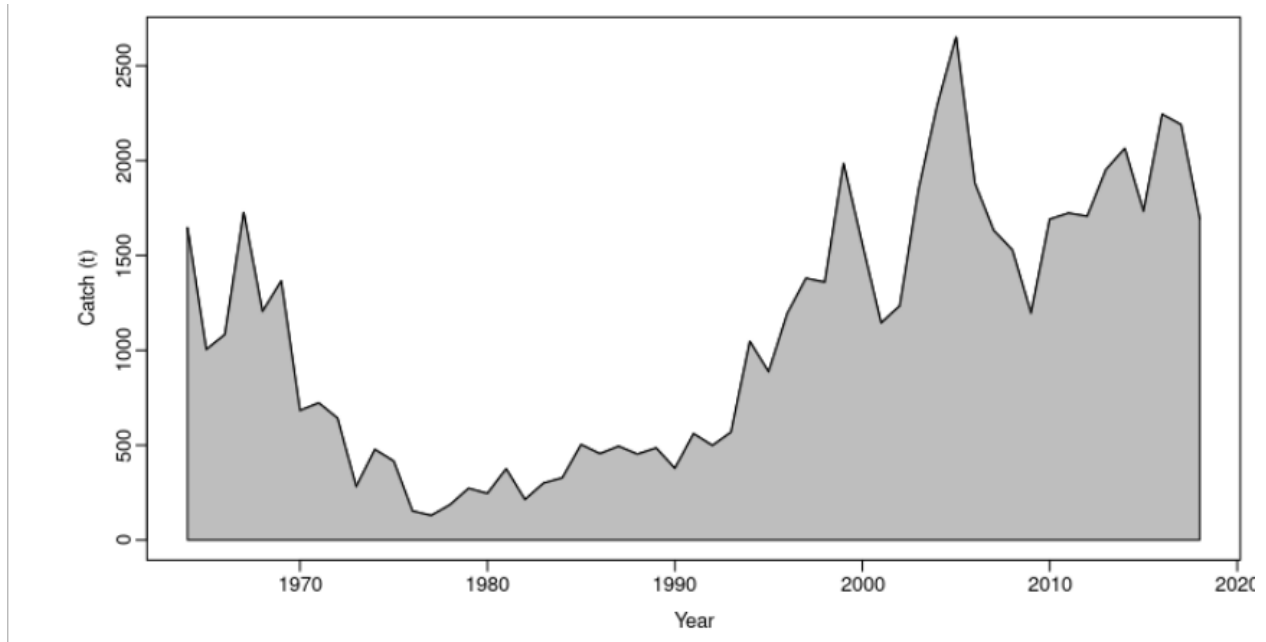
Figure A3.1: Available catch times series in metric tons (t) for Indian Ocean shortfin mako.
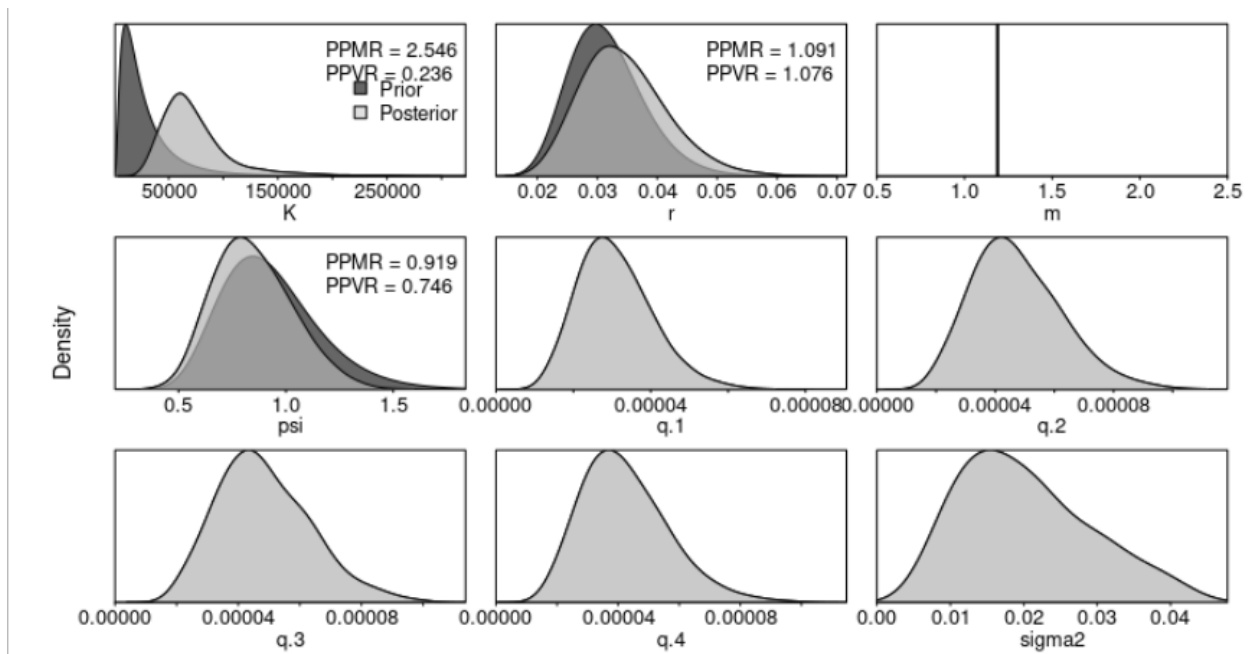
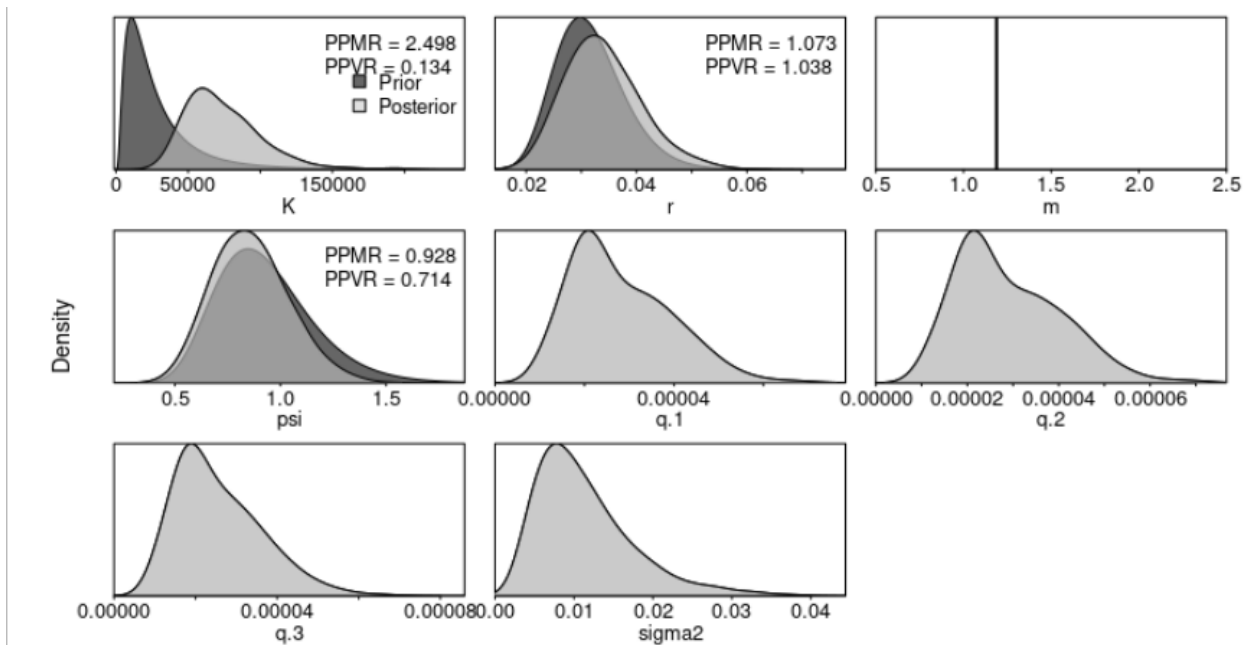Figure A3.2: Prior and posterior distributions for the JABBA model with all CPUEs. PPRM: Posterior to Prior Ratio of Means; PPRV: Posterior to Prior Ratio of Variances.
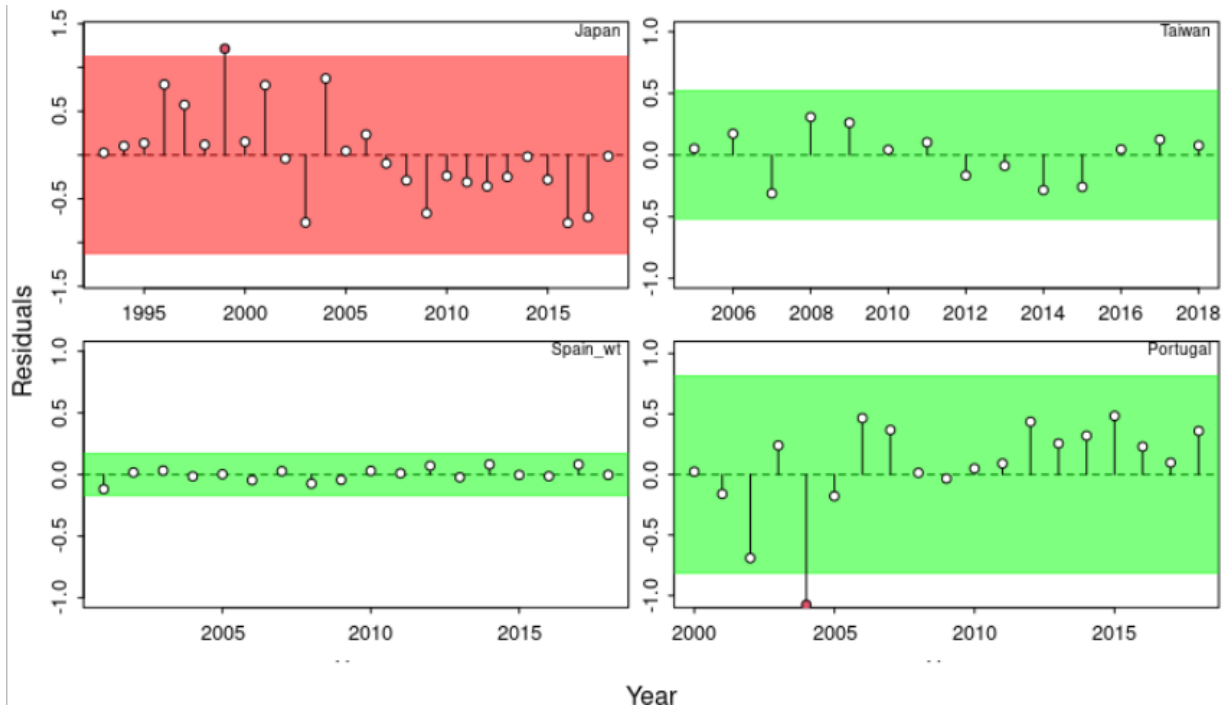
Figure A3.3: Runs tests to quantitatively evaluate the randomness of the time series of CPUE residuals by fleet for the model with all CPUEs included. Green panels indicate no evidence of lack of randomness of time series residuals (p>0.05) while red panels indicate the opposite. The inner shaded area shows three standard errors from the overall mean and red circles identify a specific year with residuals greater than this threshold value (3x sigma rule).
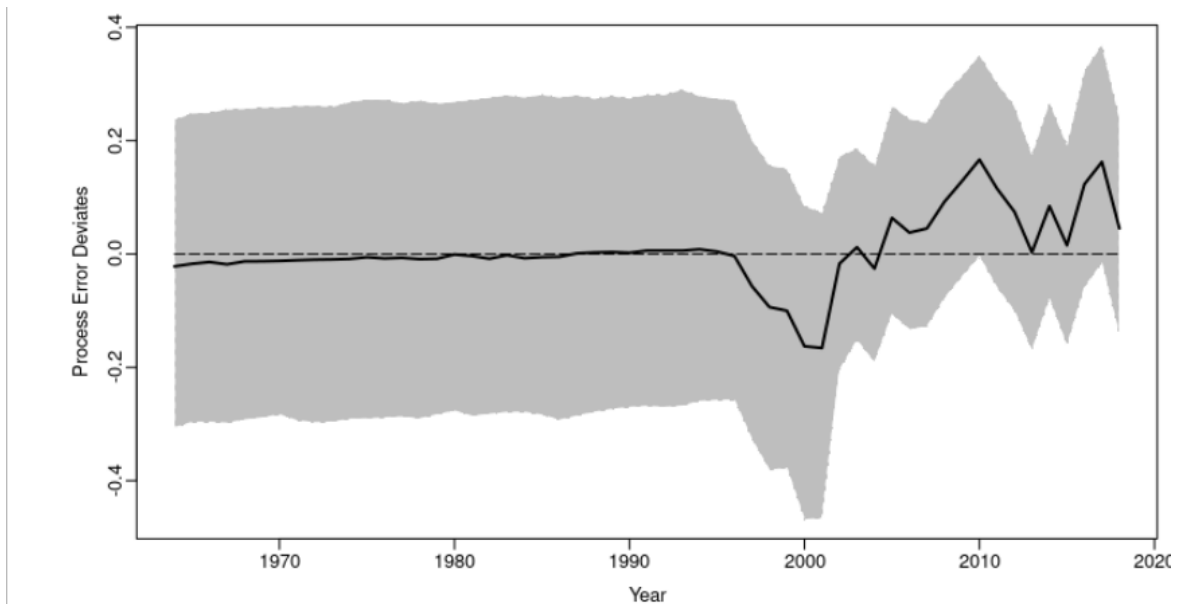
Figure A3.4: Process error deviates (median: solid line) with shaded grey area indicating 95% credibility intervals.
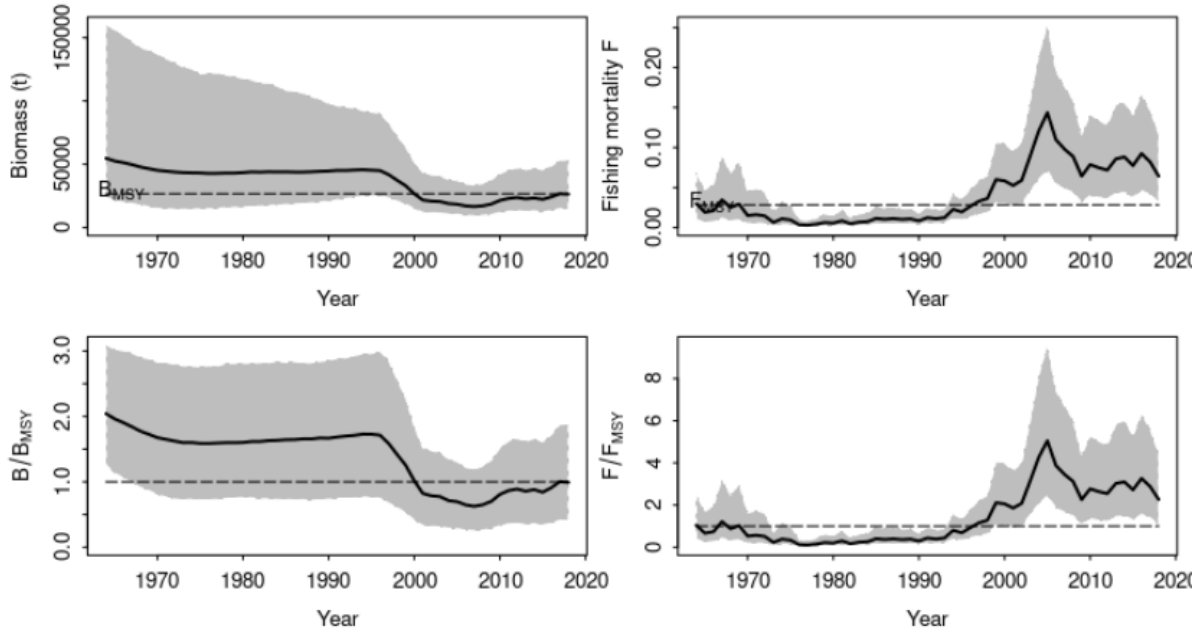
Figure A3.5: Time series of the biomass, fishing mortality, B/BMSY, and F/FMSY for the model with all CPUEs included.
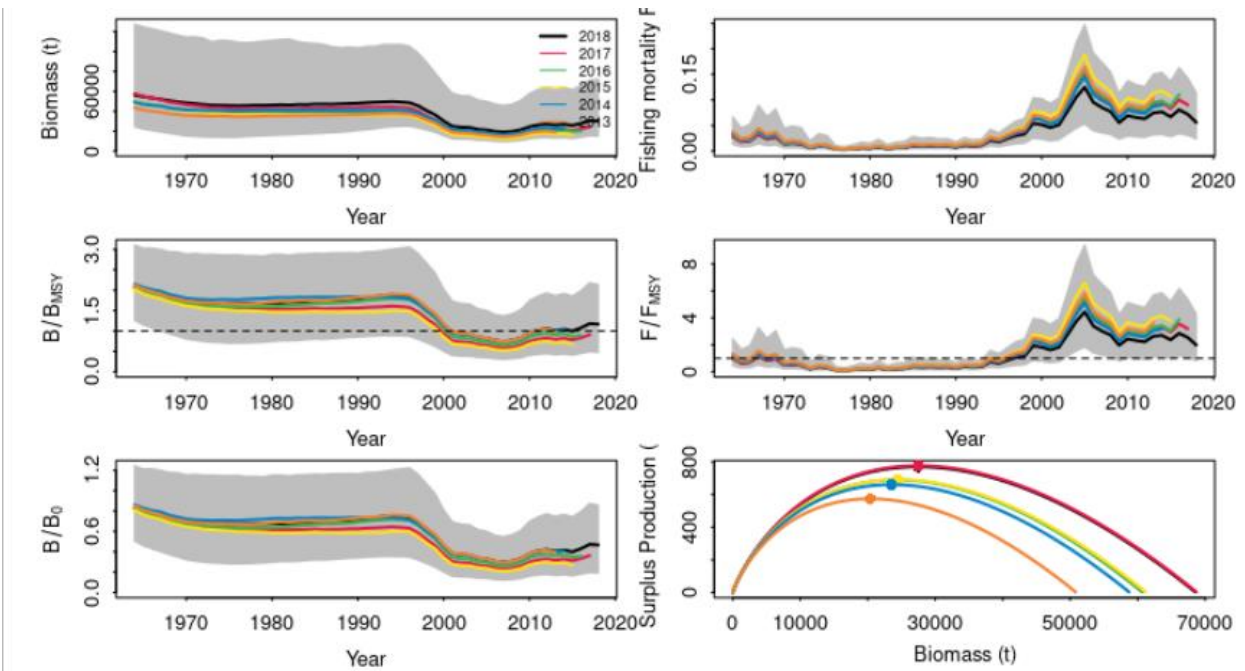
Figure A3.6: Retrospective analysis performed on the run with all CPUEs, by removing one year at a time sequentially (n=5) and predicting the trends in biomass and fishing mortality (upper panels), biomass relative to BMSY (B/BMSY) and fishing mortality relative to FMSY (F/FMSY) (middle panels) and biomass relative to K (B/K) and surplus production curve (bottom panels) for each scenario from the model fits.
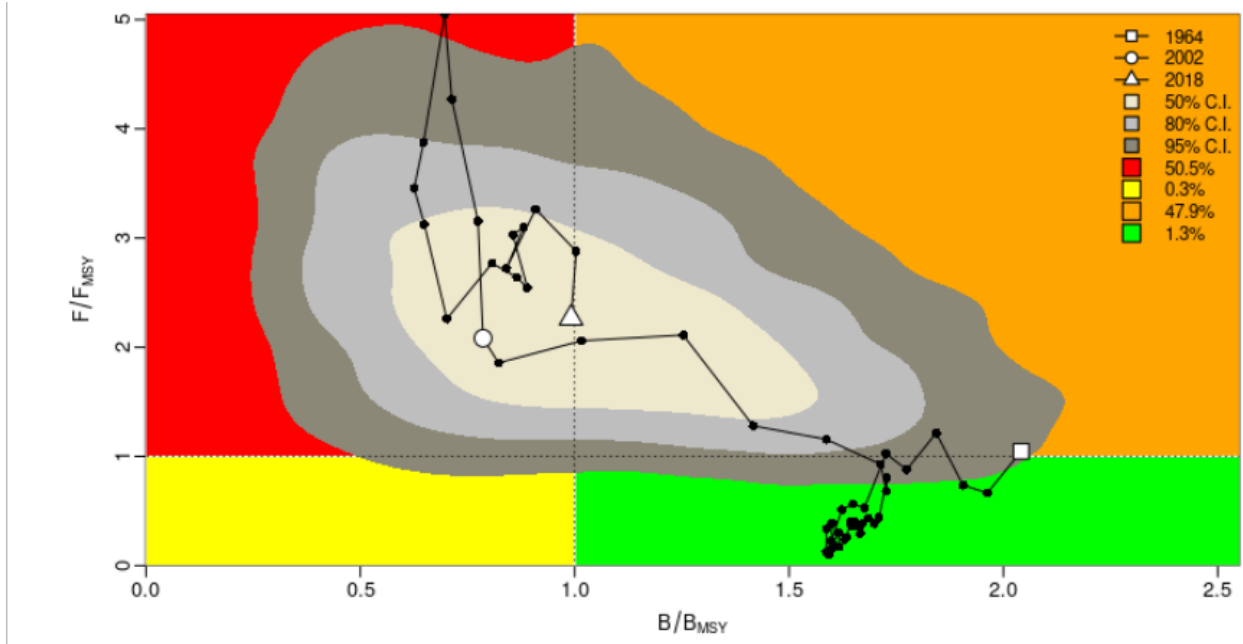
Figure A3.7: Kobe phase plot showing estimated trajectories (1963-2018) of B/BMSY and F/FMSY for the JABBA model for the Indian Ocean shortfin mako with all CPUEs. Different grey shaded areas denote the 50%, 80%, and 95% credibility interval for the terminal assessment year. The probability of terminal year points falling within each quadrant is indicated in the figure legend.

Figure A3.8: Prior and posterior distributions for the JABBA model without the Japanese CPUE time series. PPRM: Posterior to Prior Ratio of Means; PPRV: Posterior to Prior Ratio of Variances.
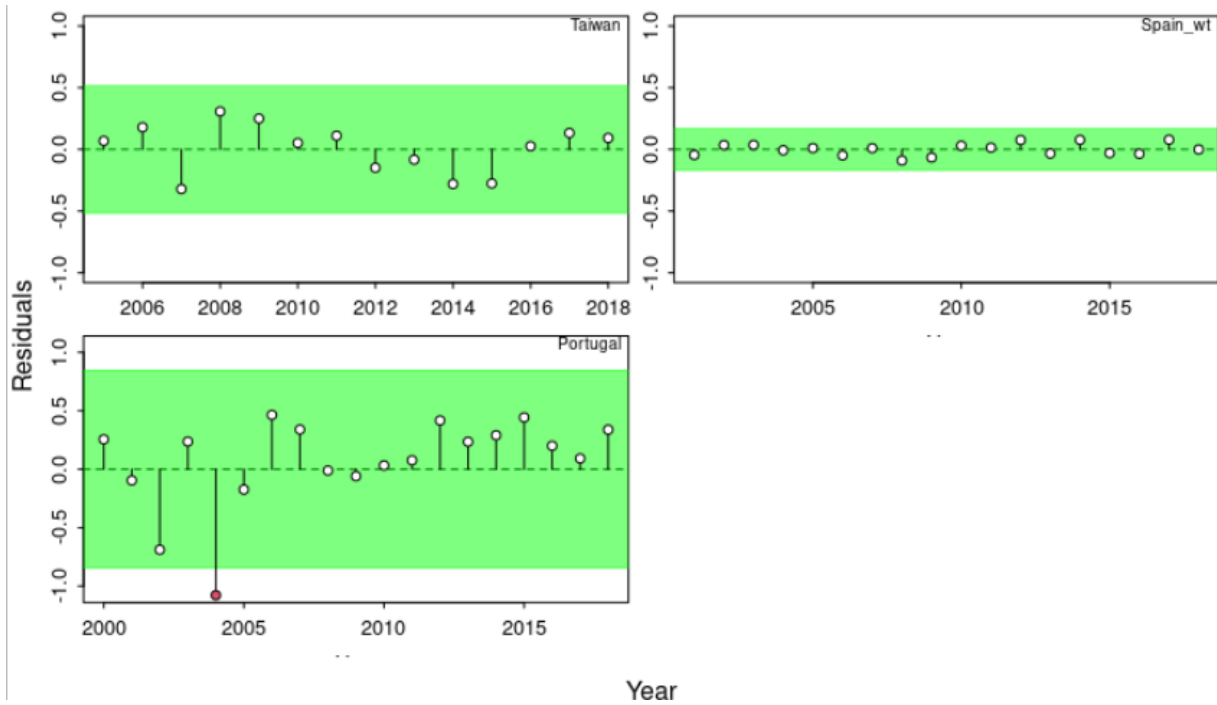
Figure A3.9: Runs tests to quantitatively evaluate the randomness of the time series of CPUE residuals by fleet for the model without the Japanese CPUE time series. Green panels indicate no evidence of lack of randomness of time series residuals (p>0.05) while red panels indicate the opposite. The inner shaded area shows three standard errors from the overall mean and red circles identify a specific year with residuals greater than this threshold value (3x sigma rule).
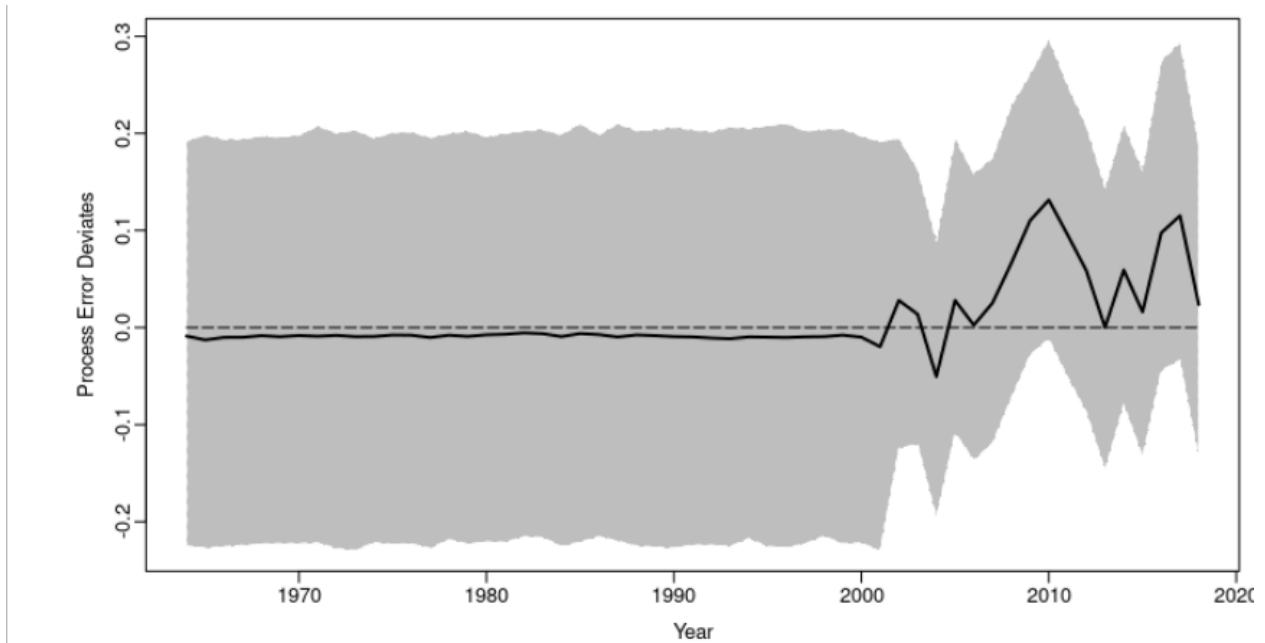

Figure A3.10: Process error deviates (median: solid line) with shaded grey area indicating 95% credibility intervals for the model without the Japanese CPUE time series.
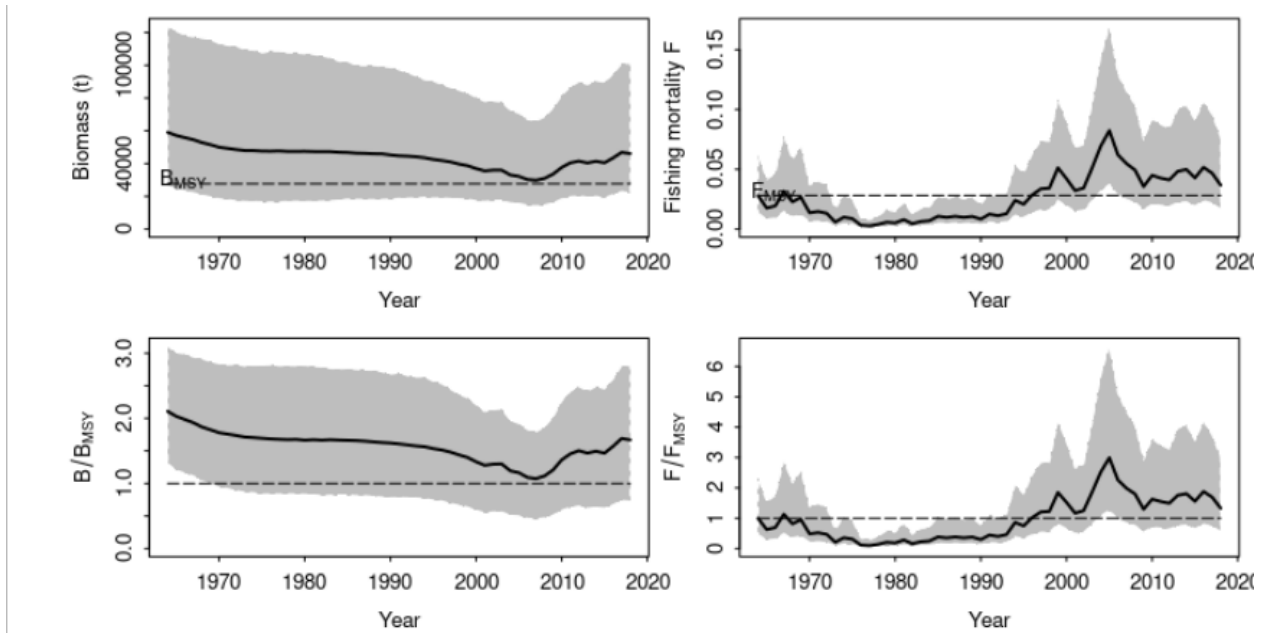
Figure A3.11: Time series of the biomass, fishing mortality, B/BMSY, and F/FMSY for the model without the Japanese CPUE time series
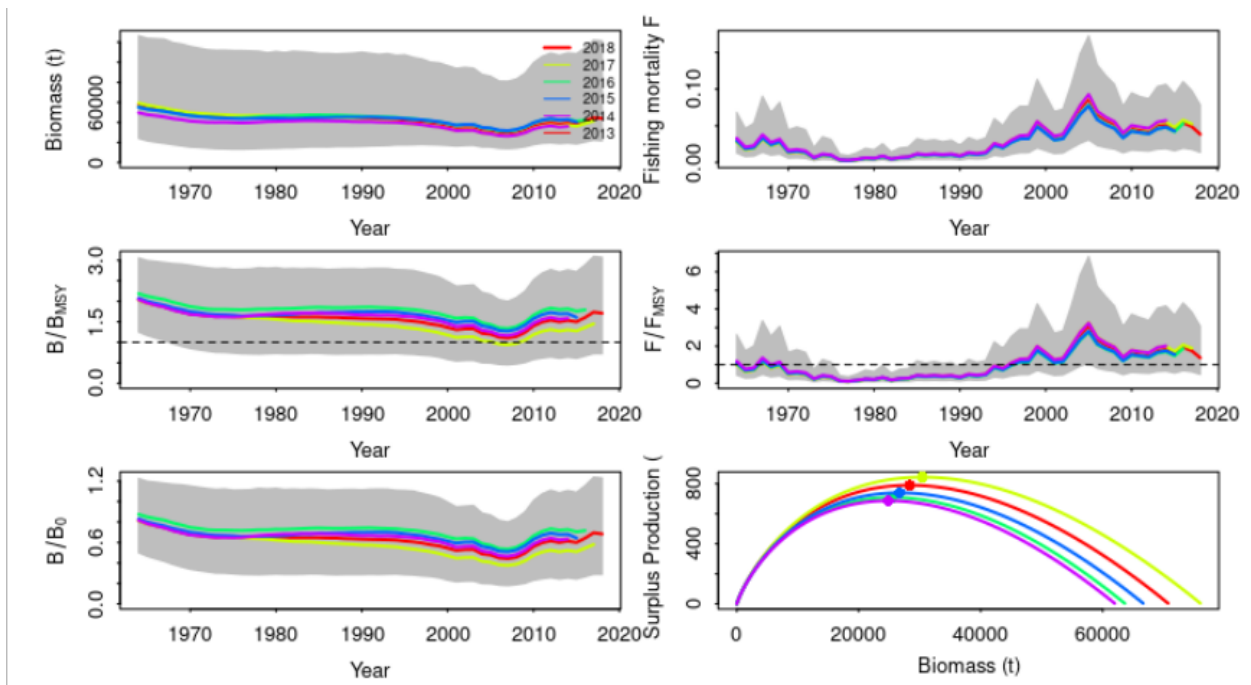

Figure A3.12: Retrospective analysis performed on the run without the Japanese CPUE time series, by removing one year at a time sequentially (n=5) and predicting the trends in biomass and fishing mortality (upper panels), biomass relative to BMSY (B/BMSY) and fishing mortality relative to FMSY (F/FMSY) (middle panels) and biomass relative to K (B/K) and surplus production curve (bottom panels) for each scenario from the model fits.
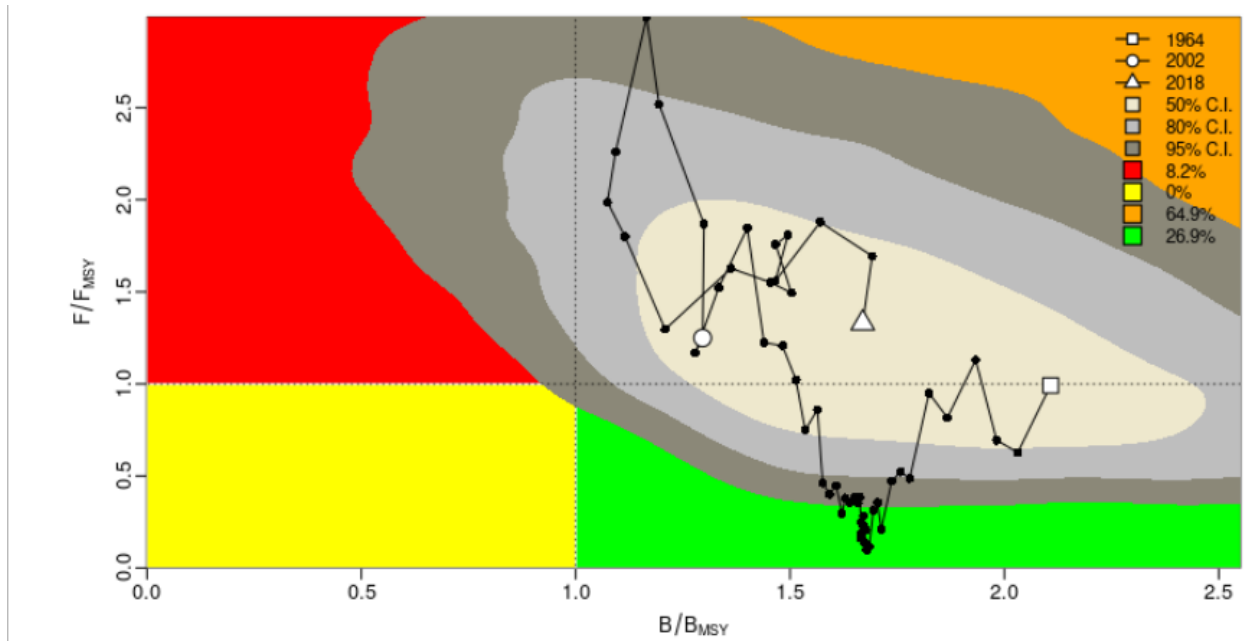
Figure A3.13: Kobe phase plot showing estimated trajectories (1963-2018) of B/BMSY and F/FMSY for the JABBA model for the Indian Ocean shortfin mako without the Japanese CPUE time series. Different grey shaded areas denote the 50%, 80%, and 95% credibility interval for the terminal assessment year. The probability of terminal year points falling within each quadrant is indicated in the figure legend.